Electronic Supplementary Material (ESI) for Green Chemistry.

SUPPORTING INFORMATION

Synthesis of urea derivatives via reductive carbon dioxide fixation into contracted porphyrin analogues

Sajal Kumar Patra, Kasturi Sahu, Bratati Patra, Dipak Kumar Sahoo, Sruti Mondal, Payel Mukherjee, Himansu S. Biswal,* and Sanjib Kar*

School of Chemical Sciences, National Institute of Science Education and Research (NISER), Bhubaneswar, Khordha, 752050, India and Homi Bhabha National Institute, Training School Complex, Anushakti Nagar, Mumbai, 400 094, India

E-mail: *himansu@niser.ac.in* and *sanjib@niser.ac.in*

Experimental Section

Materials

The precursor's pyrrole, *p*-chloranil, and aldehydes were purchased from Aldrich, USA. Ammonium carbonate (minimum 30% ammonia basis) was purchased from Qualigen fine chemicals, India. Other chemicals were of reagent grade. Hexane and CH_2Cl_2 were distilled from KOH and CaH_2 respectively. For spectroscopy studies, HPLC grade solvents were used. The synthetic methodologies and full spectroscopic characterization of **1A**-**7A** are provided in the previous literatures. [20]

Physical Measurements

UV−Vis spectral studies were performed on a Perkin−Elmer LAMBDA-**750**spectrophotometer. Emission spectral studies were performed on a Perkin Elmer, LS 55 spectrophotometer using optical cell of 1 cm path length. The elemental analyses were carried out with a Perkin−Elmer 240C elemental analyzer. FT−IR spectra were recorded on a Perkin−Elmer spectrophotometer with samples prepared as KBr pellets. The NMR measurements were carried out using a Bruker 700 MHz NMR spectrometer. Chemical shifts are expressed in parts per million (ppm) relative to residual chloroform (δ= 7.26). Electrospray mass spectra were recorded on a Bruker Micro TOF─QII mass spectrometer.

Crystal Structure Determination

Single crystals of **3B, 5B** and **7B** were grown by slow diffusion of a solution of the **3B, 5B** and **7B** in dichloromethane into hexane, followed by slow evaporation under atmospheric conditions. The crystal data of **3B, 5B** and **7B** were collected on a Bruker Kappa APEX II CCD diffractometer at 293 K. Selected data collection parameters and other crystallographic results are summarized in Table S1. All data were corrected for Lorentz polarization and absorption effects. The program package SHELXTL[25] was used for structure solution and full matrix least squares refinement on F^2. Hydrogen atoms were included in the refinement using the riding model. Contributions of H atoms for the water molecules were included but were not fixed. Disordered solvent molecules were taken out using SQUEEZE command in PLATON. [26]

CCDC 1573628-1573630 contain the supplementary crystallographic data for **3B, 5B** and **7B**. These data can be obtained free of charge via www.ccdc.cam.ac.uk/data_ request/cif.

Syntheses

Synthesis of *N*^{21}, *N*^{22}-carbamide−5,10,15−triphenylcorrole, 1B:

The carbamide-corrole (**1B−8B**) were prepared by following a general procedure. Hence, only one representative case is discussed below. 0.050 g (0.095 mmol) of 5,10,15−triphenylcorrole, **1A** was dissolved in 30 mL of dry dichloromethane and subsequently 4.0 g of $(NH_4)_2CO_3$ was added to the reaction mixture in stirring condition. After 5 minutes, 50 mL of pyridine was added and the reaction mixture was refluxed for 3 h at around 110ºC. Then the mixture was evaporated to dryness by rotary evaporation. It was kept for recrystallization in a dichloromethane/hexane mixture for overnight. The residual solvent mixture including the solid mass was dried by rotary evaporation and the reddish colored crude product was purified by using column chromatography through a silica gel (100-200 mesh) bed and by using 55% dichloromethane and 45% hexane as eluent.

For *N*^{21}, *N*^{22}-carbamide−5,10,15−triphenylcorrole, 1B:

Yield: 58% (30 mg). Anal. Calcd (found) for $C_{38}H_{24}N_4O$ (**1B**): C, 82.59 (82.68); H, 4.38 (4.31); N, 10.14 (10.25). λ_{max}/nm (ε/$M^{-1}cm^{-1}$) in toluene: 407 (131000), 425sh (80000), 508 (9800), 540 (17500), 566 (9500), 615 (10000). ^{1}H NMR (700 MHz, $CDCl_3$) δ 9.55 (d, *J* = 4.4 Hz, 1H), 8.95 (d, *J* = 4.1 Hz, 1H), 8.79 (d, *J* = 4.2 Hz, 1H), 8.73 (d, *J* = 5.1 Hz, 1H), 8.60 (dd, *J* = 4.4, 2.4 Hz, 2H), 8.58 (d, *J* = 5.1 Hz, 1H), 8.36 (d, *J* = 7.4 Hz, 1H), 8.32 – 8.22 (m, 5H), 8.03 (d, *J* = 7.4 Hz, 1H), 7.86 – 7.75 (m, 6H), 7.75 – 7.68 (m, 3H). (Fig. S1). ^{13}C NMR (176 MHz, $CDCl_3$) δ 143.31, 143.16, 142.85, 142.42, 139.19, 138.88, 136.20, 135.86, 134.82, 134.20, 134.08, 132.87, 132.80, 130.54, 130.26, 129.45, 129.37, 129.21, 128.48, 128.29, 128.18, 127.80, 127.56, 127.38, 127.25, 126.24, 125.49, 124.63, 123.62, 121.08, 120.24, 118.95, 116.67, 115.99, 115.29, 114.22, 111.19, 109.78 (Fig. S2). **1B** displayed strong fluorescence at 633 nm and a shoulder at 681 nm in toluene. The electrospray mass spectrum in methanol showed peaks centred at *m/z* = 553.20 correspond to [**1B+H**]$^+$ (552.20 calcd for $C_{38}H_{24}N_4O$) {Fig. S33}.

For N^{21}, N^{22} carbamide−10−(2,4,5−trimethoxyphenyl)−5,15−bis(4−cyanophenyl)corrole, 2B:

Yield: 62% (32 mg). Anal. Calcd (found) for $C_{43}H_{28}N_6O_4$ (**2B**): C, 74.56 (74.67); H, 4.07 (4.15); N, 12.13 (12.22). λ_{max}/nm (ε/$M^{-1}cm^{-1}$) in toluene: 416 (145,000), 508 (12000), 545 (23000), 576 (12500), 622 (14000). ^{1}H NMR (700 MHz, $CDCl_3$) δ 9.55 (d, *J* = 23.3 Hz, 1H), 9.05 – 8.88 (m, 2H), 8.67-8.45 (m, 5H), 8.36 (d, *J* = 24.3 Hz, 4H), 8.07 (d, *J* = 26.9 Hz, 3H), 7.79 (s, 1H), 7.41 (s, 1H), 7.02 (m, 1H), 4.20- 3.98 (m,5H), 3.86 (s, 2H), 3.71 (s, 1H), 3.32 (s, 1H) (Fig. S3). **2B** displayed strong fluorescence at 641 nm and a shoulder at 689 nm in toluene. The electrospray mass spectrum in methanol showed peaks centered at *m/z* = 693.13 correspond to [**2B+H**] $^+$ (692.22 calcd for $C_{43}H_{28}N_6O_4$) (Fig. S34).

For N^{21}, N^{22}-carbamide−10− (4,7−dimethoxynaphthalen-1-yl)-5,15-bis(4-cyanophenyl)corrole, 3B:

Yield: 65% (34 mg). Anal. Calcd (found) for $C_{46}H_{28}N_6O_3$ (**3B**): C, 77.52 (77.64); H, 3.96 (3.87); N, 11.79 (11.87). λ_{max}/nm (ε/$M^{-1}cm^{-1}$) in toluene: 417 (93,000), 512 (3500), 545 (10500), 576 (3600), 622 (5500). ^{1}H NMR (700 MHz, $CDCl_3$) δ 9.64 (dd, *J* = 13.4, 4.5 Hz, 1H), 9.03 (dd, *J* = 24.1, 4.2 Hz, 1H), 8.78 (dd, *J* = 32.2, 4.7 Hz, 1H), 8.71 (dd, *J* = 10.6, 4.7 Hz, 1H), 8.61 (dd, *J* = 17.4, 4.5 Hz, 1H), 8.54 – 8.45 (m, 2H), 8.44 – 8.29 (m, 5H), 8.17 – 8.04 (m, 4H), 7.89 (d, *J* = 7.7 Hz, 1H), 7.23 – 7.18 (m, 1H), 7.06 – 6.97 (m, 1H), 6.58 (d, *J* = 2.5 Hz, 1H), 6.02 (d, *J* = 2.5 Hz, 1H), 4.29 (s, 1H), 4.24 (s, 2H), 2.99 (s, 2H), 2.64 (s, 1H) (Fig. S4). **3B** displayed strong fluorescence at 640 nm and a shoulder at 690 nm in toluene. The electrospray mass spectrum in methanol showed peaks centered at m/z = 713.23 correspond to [**3B+H**] $^+$ (712.22 calcd for $C_{46}H_{28}N_6O_3$) (Fig. S35).

For N^{21}, N^{22}-carbamide−5,10,15−tris(4-Benzyloxyphenyl)corrole, 4B:

Yield: 55% (28 mg). Anal. Calcd (found) for $C_{59}H_{42}N_4O_4$ (**4B**): C, 81.36 (81.48); H, 4.86 (4.98); N, 6.43 (6.35). λ_{max}/nm (ε/$M^{-1}cm^{-1}$) in toluene: 413 (93,000), 429sh (49,000), 509 (4000), 544 (9000), 571 (4500), 619 (5000). ^{1}H NMR (700 MHz, $CDCl_3$) δ 9.50 (d, *J* = 4.3 Hz, 1H), 8.91 (d, *J* = 4.1 Hz, 1H), 8.77 (d, *J* = 4.1 Hz, 1H), 8.72 (d, *J* = 5.0 Hz, 1H), 8.57 (d, *J* = 4.3 Hz, 1H), 8.55 (d, *J* = 4.3 Hz, 1H), 8.53 (d, *J* = 5.1 Hz, 1H), 8.30 (d, *J* = 4.3 Hz, 1H), 8.27 (d, *J* = 8.1 Hz, 1H), 8.20 (d, *J* = 8.0 Hz, 1H), 8.18 – 8.15 (m, 2H), 7.94 (d, *J* = 8.2 Hz, 1H), 7.63 (d, *J* = 7.5 Hz, 2H), 7.60 (dd, *J* = 7.5, 4.9 Hz, 4H), 7.49 (td, *J* = 7.9, 2.1 Hz, 7H), 7.42 (q, *J* = 7.9, 7.4

Hz, 9H), 5.35 (bs, 2H), 5.32 (bs, 4H). (Fig. S5). **4B** displayed strong fluorescence at 642 nm and a shoulder at 692 nm in toluene. The electrospray mass spectrum in methanol showed peaks centered at *m/z* = 871.37 correspond to [**4B+H**] $^{+}$ (870.32 calcd for $C_{59}H_{42}N_4O_4$) (Fig. S36).

For *N*^{21}, *N*^{22}-carbamide−5,10,15−tris(4-cyanophenyl)corrole, 5B:

Yield: 70% (36 mg). Anal. Calcd (found) for $C_{41}H_{21}N_7O$ (**5B**): C, 78.46 (78.33); H, 3.37 (3.49); N, 15.62 (15.69). λ_{max}/nm (ε/$M^{-1}cm^{-1}$) in toluene: 415 (90,000), 509 (3100), 543 (8500), 572 (2500), 620 (2600). ^{1}H NMR (700 MHz, $CDCl_3$) δ 9.68 (d, *J* = 4.4 Hz, 1H), 9.05 (d, *J* = 4.2 Hz, 1H), 8.77 (d, *J* = 4.2 Hz, 1H), 8.73 (d, *J* = 5.1 Hz, 1H), 8.66 (d, *J* = 4.4 Hz, 1H), 8.62 (d, *J* = 5.1 Hz, 1H), 8.57 (d, *J* = 4.4 Hz, 1H), 8.50 (d, *J* = 7.8 Hz, 1H), 8.41 (d, *J* = 7.5 Hz, 1H), 8.37 (d, *J* = 7.6 Hz, 2H), 8.26 (d, *J* = 4.4 Hz, 1H), 8.15 (t, *J* = 6.8 Hz, 3H), 8.09 (d, *J* = 7.8 Hz, 2H), 8.03 (d, *J* = 7.7 Hz, 1H), 7.96 (d, *J* = 8.0 Hz, 1H), 7.78 (d, *J* = 8.1 Hz, 1H) (Fig. S6). ^{13}C NMR (176 MHz, $CDCl_3$) δ 147.33, 143.60, 142.83, 142.73, 142.07, 140.45, 138.33, 136.51, 135.24, 134.71, 134.39, 133.64, 133.48, 133.06, 132.35, 132.06, 131.49, 130.67, 130.23, 129.86, 129.45, 127.67, 126.40, 126.34, 125.83, 122.37, 122.02, 121.66, 120.06, 119.09, 118.93, 118.75, 118.27, 115.34, 115.20, 112.69, 112.65, 111.85, 111.77, 108.33. (Fig. S7). **5B** displayed strong fluorescence at 640 nm and a shoulder at 696 nm in toluene. The electrospray mass spectrum in methanol showed peaks centered at *m/z* = 628.58 correspond to [**5B+H**] $^{+}$ (627.18 calcd for $C_{41}H_{21}N_7O$) (Fig. S37).

For *N*^{21}, *N*^{22}-carbamide−5,10,15−tris(2-bromo-5-fluoro-phenyl)corrole, 6B:

Yield: 60% (31 mg). Anal. Calcd (found) for $C_{38}H_{18}Br_3F_3N_4O$ (**6B**): C, 54.12 (54.02); H, 2.15 (2.26); N, 6.64 (6.72). λ_{max}/nm (ε/$M^{-1}cm^{-1}$) in toluene: 405 (142,000), 420sh (103,000), 501 (9900), 536 (19000), 564 (7600), 613 (8400). ^{1}H NMR (700 MHz, $CDCl_3$) δ 9.58 (tq, *J* = 9.1, 4.3 Hz, 1H), 8.99 – 8.87 (m, 1H), 8.78 – 8.50 (m, 2H), 8.46 – 8.33 (m, 3H), 8.24 – 7.73 (m, 6H), 7.46 – 7.30 (m, 3H), 7.22 – 7.10 (m, 1H) (Fig. S8). **6B** displayed strong fluorescence at 624 nm and a shoulder at 676 nm in toluene. The electrospray mass spectrum in methanol showed peaks centered at *m/z* = 844.90 correspond to [**6B+H**] $^{+}$ (843.89 calcd for $C_{38}H_{18}Br_3F_3N_4O$) (Fig. S38).

For *N*^{21}, *N*^{22}-carbamide−5,10,15−tris(4-nitrophenyl)corrole, 7B:

Yield: 60% (31 mg). Anal. Calcd (found) for $C_{38}H_{21}N_7O_7$ (**7B**): C, 66.38 (66.49); H, 3.08 (3.15); N, 14.26 (14.37). λ_{max}/nm ($\varepsilon/M^{-1}cm^{-1}$) in dichloromethane: 432 (68,000), 515 (7600), 550 (11000), 578 (7000), 627 (7500). ^{1}H NMR (700 MHz, $CDCl_3$) δ 9.71 (d, *J* = 3.9 Hz, 1H), 9.08 (d, *J* = 3.8 Hz, 1H), 8.79 (s, 1H), 8.74 (dd, *J* = 22.7, 6.5 Hz, 4H), 8.71 – 8.63 (m, 4H), 8.62-8.53 (m, 3H), 8.49 (s, 2H), 8.43 (d, *J* = 7.8 Hz, 2H), 8.29 (s, 1H), 8.23 (d, *J* = 7.0 Hz, 1H) (Fig. S9). **7B** displayed strong fluorescence at 652 nm and a shoulder at 712 nm in toluene. The electrospray mass spectrum in methanol showed peaks centred at *m/z* = 688.55 correspond to [**7B+H**]$^+$ (687.15 calcd for $C_{38}H_{21}N_7O_7$) (Fig. S39).

Computational Methods:

Geometry optimizations of **1B-7B** were carried out using Grimme's functional including dispersion i.e. at B97D/6-31G*[27] level as implemented in Turbomole[28] software. B97D not only accounts for dispersive attraction but also provides reliable spectroscopic parameters that match with the experimental data (vide infra).[29] Vibrational frequency calculations were also performed at the same level to ensure the optimized structures are the true minima. The vibrational frequencies were scaled by 0.972 to account for the anharmonicity. The TD-DFT calculation was performed at the TD-B97D/6-31G* level to obtain electronic transitions. Gaussian09[30] software was used for the TD-DFT computation.

Notes and references

25. G. M. Sheldrick, *Acta Crystallogr., Sect. A: Found. Crystallogr.*, 2008, **64**, 112-122.

26. P. Van der Sluis and A. Spek, *Acta Crystallogr., Sect. A: Found. Crystallogr.*, 1990, **46**, 194-201.

27. S. Grimme*, J. Comput. Chem.,* 2006*,* **27,** 1787-1799.

28. F. Furche, R. Ahlrichs, C. Hättig, W. Klopper, M. Sierka, and F. Weigend, *WIREs Comput. Mol. Sci.* 2014**, 4**, 91-100.

29. V. R. Mundlapati, S. Gautam, D. K. Sahoo, A. Ghosh and H. S. Biswal, *J. Phys. Chem. Lett.*, 2017, **8**, 4573-4579

30. M. J. Frisch, G. W. Trucks, H. B. Schlegel, G. E. Scuseria, M. A. Robb, J. R. Cheeseman, G. Scalmani, V. Barone, B. Mennucci, etal. et al. *Gaussian 09, Revision C.01*; Gaussian, Inc.: Wallingford, CT, **2011**.

Table S1 Crystallographic Data for **3B, 5B** and **7B**.

compound codes	**3B**	**5B**	**7B**
molecular formula	$C_{46}H_{28}N_6O_3$	$C_{41}H_{21}N_7O$	$C_{38}H_{21}N_7O_7$
Fw	712.74	627.65	687.62
Radiation	MoKα	MoKα	Mo *K*α
crystal symmetry	Triclinic	Triclinic	Monoclinic
space group	P-1	P-1	$P2_1/c$
a(Å)	7.2077 (11)	7.7014 (5)	16.1335 (8)
b(Å)	17.214 (3)	15.7670 (9)	16.7689 (8)
c(Å)	18.628 (3)	17.5273 (10)	13.7048 (6)
α(deg)	116.909 (8)	115.061 (4)	90
β(deg)	91.456 (9)	98.474 (4)	111.276 (2)
γ(deg)	101.060 (9)	93.397 (4)	90
V(Å^3)	2006.0 (6)	1889.2 (2)	3455.0 (3)
Z	2	2	4
μ (mm^{-1})	0.08	0.07	0.09
T(K)	296	296	296
D_{calcd} (g cm^{-3})	1.180	1.103	1.322
2θ range (deg)	4.45 to 50.83	4.74 to 51.69	3.64 to 52.18
e data (R_{int})	7371 (0.087)	7236 (0.071)	6826 (0.093)
R1 ($I>2\sigma(I)$)	0.070	0.085	0.064
WR2 (all data)	0.176	0.268	0.183
GOF	0.99	0.98	0.96
$\Delta\rho_{max}$, $\Delta\rho_{min}$ (e Å^{-3})	0.76, −0.32	0.89, −0.49	0.48, −0.31

Table S2 UV–Vis. Data [a, b]

Compound	UV–vis. Data [a,b] λ_{max} / nm (ε / $M^{-1}cm^{-1}$)
1B [a]	407 (131,000), 425sh (80000), 508 (9800), 540 (17500), 566 (9500), 615 (10000)
2B [a]	416 (145,000), 508 (12000), 545 (23000), 576 (12500), 622 (14000)
3B [a]	417 (93,000), 512 (3500), 545 (10500), 576 (3600), 622 (5500)
4B [a]	413 (93,000), 429sh (49,000), 509 (4000), 544 (9000), 571 (4500), 619 (5000)
5B [a]	415 (90,000), 509 (3100), 543 (8500), 572 (2500), 620 (2600)
6B [a]	405 (142,000), 420sh (103,000), 501 (9900), 536 (19000), 564 (7600), 613 (8400)
7B [b]	432 (68,000), 515 (7600), 550 (11000), 578 (7000), 627 (7500)

[a] In toluene

[b] In dichloromethane

Table S3. Selected X-ray and DFT calculated (B97-D/6-31G*) bond distances (Å) and angles (deg) for 7B.

Number denotes atoms R= distance A= Angles	**7B** (X-ray)	**7B** B97-D/6-31G*
R(1-35)	1.211	1.213
R(2-9)	1.377	1.378
R(2-10)	1.357	1.371
R(3-17)	1.371	1.368
R(3-29)	1.357	1.348
R(4-20)	1.384	1.412
R(4-23)	1.396	1.411
R(4-35)	1.404	1.426
R(5-13)	1.409	1.424
R(5-28)	1.407	1.421
R(5-35)	1.433	1.417
R(6-7)	1.209	1.238
R(6-8)	1.227	1.238
R(6-33)	1.483	1.484
R(9-16)	1.411	1.433
R(9-25)	1.429	1.439
R(10-15)	1.411	1.424
R(10-24)	1.42	1.447
R(11-12)	1.214	1.238
R(11-18)	1.214	1.238
R(11-38)	1.469	1.484
R(13-15)	1.402	1.424
R(13-45)	1.418	1.435
R(14-15)	1.5	1.498
R(14-27)	1.378	1.413
R(14-43)	1.392	1.413
R(16-17)	1.409	1.424
R(16-21)	1.469	1.482
R(17-32)	1.449	1.465
R(19-36)	1.22	1.238
R(19-39)	1.473	1.486
R(19-44)	1.212	1.238
R(20-29)	1.425	1.424

R(20-41)	1.395	1.414
R(21-22)	1.388	1.416
R(21-42)	1.386	1.416
R(22-30)	1.372	1.397
R(23-31)	1.408	1.415
R(23-37)	1.386	1.419
R(24-25)	1.348	1.386
R(26-31)	1.498	1.48
R(26-46)	1.371	1.416
R(26-51)	1.368	1.416
R(27-48)	1.394	1.398
R(28-31)	1.396	1.41
R(28-49)	1.387	1.42
R(29-40)	1.424	1.458
R(30-38)	1.371	1.402
R(32-40)	1.346	1.379
R(33-34)	1.364	1.402
R(33-47)	1.362	1.402
R(34-51)	1.385	1.397
R(37-41)	1.38	1.401
R(38-50)	1.366	1.402
R(39-48)	1.371	1.401
R(39-52)	1.381	1.402
R(42-50)	1.382	1.397
R(43-52)	1.363	1.398
R(45-49)	1.366	1.385
R(46-47)	1.393	1.397
A(1-35-4)	127.6	126.1
A(1-35-5)	122.4	124.3
A(9-2-10)	111.9	112.1
A(2-9-16)	121.9	121.2
A(2-9-25)	105.3	106.1
A(2-10-15)	126.6	126.7
A(2-10-24)	105.2	105.5
A(17-3-29)	108.3	108
A(3-17-16)	119.7	120.3
A(3-17-32)	107.6	108.9
A(3-29-20)	116.7	117.5
A(3-29-40)	109	110.3
A(20-4-23)	109.4	109.7
A(20-4-35)	126.6	127
A(4-20-29)	119.4	119.3
A(4-20-41)	106.3	106.2
A(23-4-35)	121.4	121.2
A(4-23-31)	117.2	118.4
A(4-23-37)	107	106.4

A(4-35-5)	110	109.6
A(13-5-28)	110.4	110
A(13-5-35)	128.6	128
A(5-13-15)	129.9	130.6
A(5-13-45)	104.2	104.7
A(28-5-35)	118.4	119.6
A(5-28-31)	120.3	120.7
A(5-28-49)	106.1	106.6
A(7-6-8)	124.6	125
A(7-6-33)	117.8	117.5
A(8-6-33)	117.6	117.5
A(6-33-34)	119.4	119.1
A(6-33-47)	118.2	119.1
A(16-9-25)	132.5	132.4
A(9-16-17)	119.5	120.3
A(9-16-21)	120.2	120.2
A(9-25-24)	107.8	107.7
A(15-10-24)	128.2	127.9
A(10-15-13)	130.6	130.7
A(10-15-14)	115.6	115.2
A(10-24-25)	109.7	108.4
A(12-11-18)	123.1	125
A(12-11-38)	119	117.5
A(18-11-38)	117.9	117.5
A(11-38-30)	118.9	119.1
A(11-38-50)	118.7	119.1
A(15-13-45)	125.3	124
A(13-15-14)	113.7	114
A(13-45-49)	110	110.3
A(15-14-27)	121.6	120.8
A(15-14-43)	120.3	120.3
A(27-14-43)	118.1	118.9
A(14-27-48)	121.3	120.9
A(14-43-52)	121.7	120.9
A(17-16-21)	120.3	119.3
A(16-17-32)	131.8	129.9
A(16-21-22)	120.3	119.7
A(16-21-42)	121.7	121.7
A(17-32-40)	107.4	106.6
A(36-19-39)	118.7	117.5
A(36-19-44)	124.5	125.1
A(39-19-44)	116.8	117.5
A(19-39-48)	119.8	119
A(19-39-52)	118.4	119.1
A(29-20-41)	132.8	132.6
A(20-29-40)	134.4	132.1

A(20-41-37)	109.2	109.1
A(22-21-42)	118	118.6
A(21-22-30)	121.7	121.1
A(21-42-50)	121	121
A(22-30-38)	118.3	118.8
A(31-23-37)	135.8	135.1
A(23-31-26)	121.9	121.9
A(23-31-28)	118.5	117.2
A(23-37-41)	108.1	108.3
A(31-26-46)	119.2	120.6
A(31-26-51)	122.4	120.8
A(26-31-28)	119.5	120.9
A(46-26-51)	118.3	118.6
A(26-46-47)	121.6	121
A(26-51-34)	121.6	121
A(27-48-39)	118.2	118.7
A(31-28-49)	133.5	132.7
A(28-49-45)	109.4	108.4
A(29-40-32)	107.7	106
A(30-38-50)	122.3	121.8
A(34-33-47)	122.3	121.7
A(33-34-51)	118.3	118.9
A(33-47-46)	117.9	118.8
A(38-50-42)	118.6	118.9
A(48-39-52)	121.8	121.9
A(39-52-43)	118.7	118.7

Table S4. A comparison of experimental and computed UV-Vis transitions of 1B-7B.

Compound	UV−vis. data λ_{max} / nm (Experimental)	UV−vis. data λ_{max} / nm (Theory)
1B	408, 424	418, 442
2B	413	427
3B	418	438, 470
4B	413, 429	433, 444
5B	416	415, 468
6B	405, 420	420, 434
7B	432	415

Table S5. A comparison of experimental and computed CO stretching frequencies of 1B-7B. A scaling factor of 0.972 is used for the computed vibrational frequencies.

Compound	CO stretching freq. (cm^{-1}) (Experimental)	CO stretching freq. (cm^{-1}) (Theory)
1B	1736	1733
2B	1735	1721
3B	1737	1719
4B	1724	1734
5B	1737	1737
6B	1742	1740
7B	1734	1737

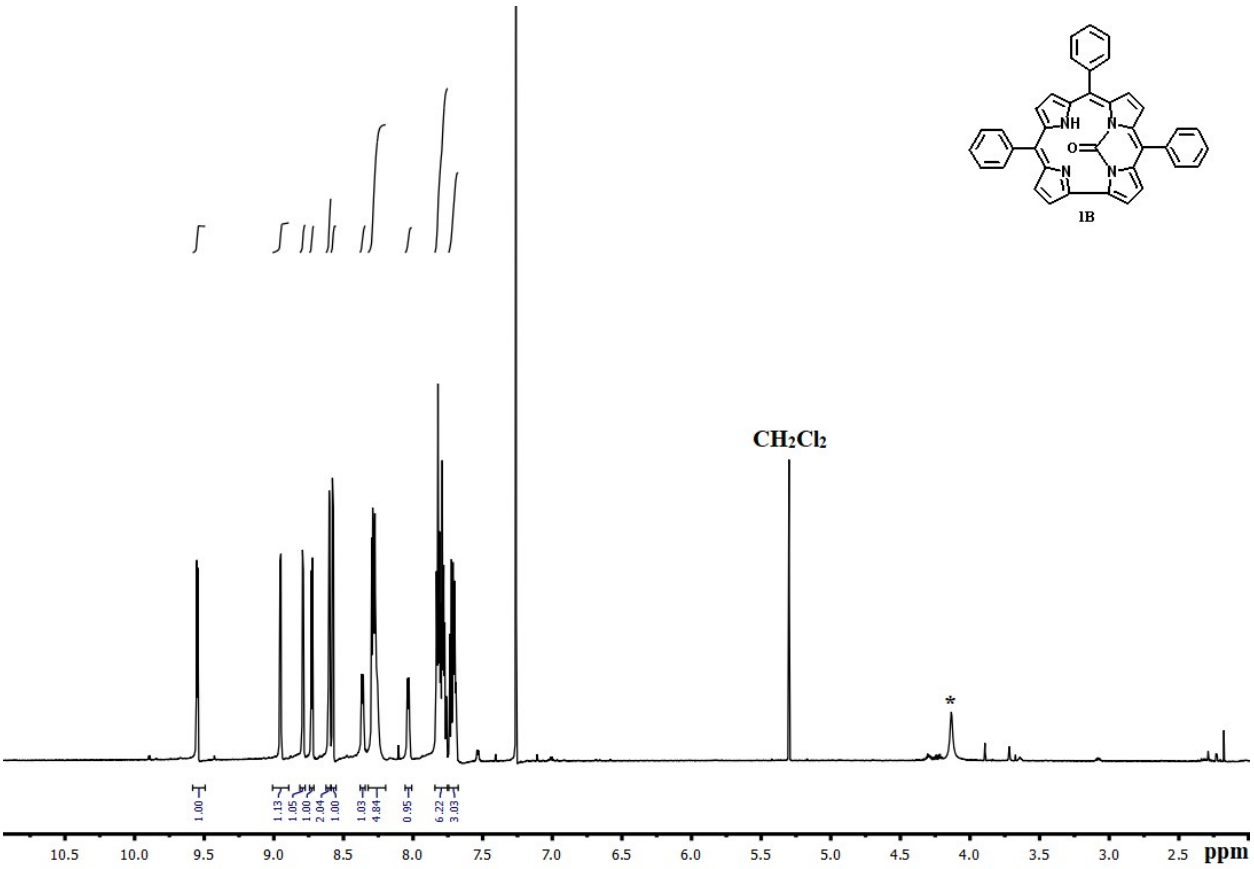

Fig. S1. ^{1}H NMR spectrum of **1B** in $CDCl_3$.

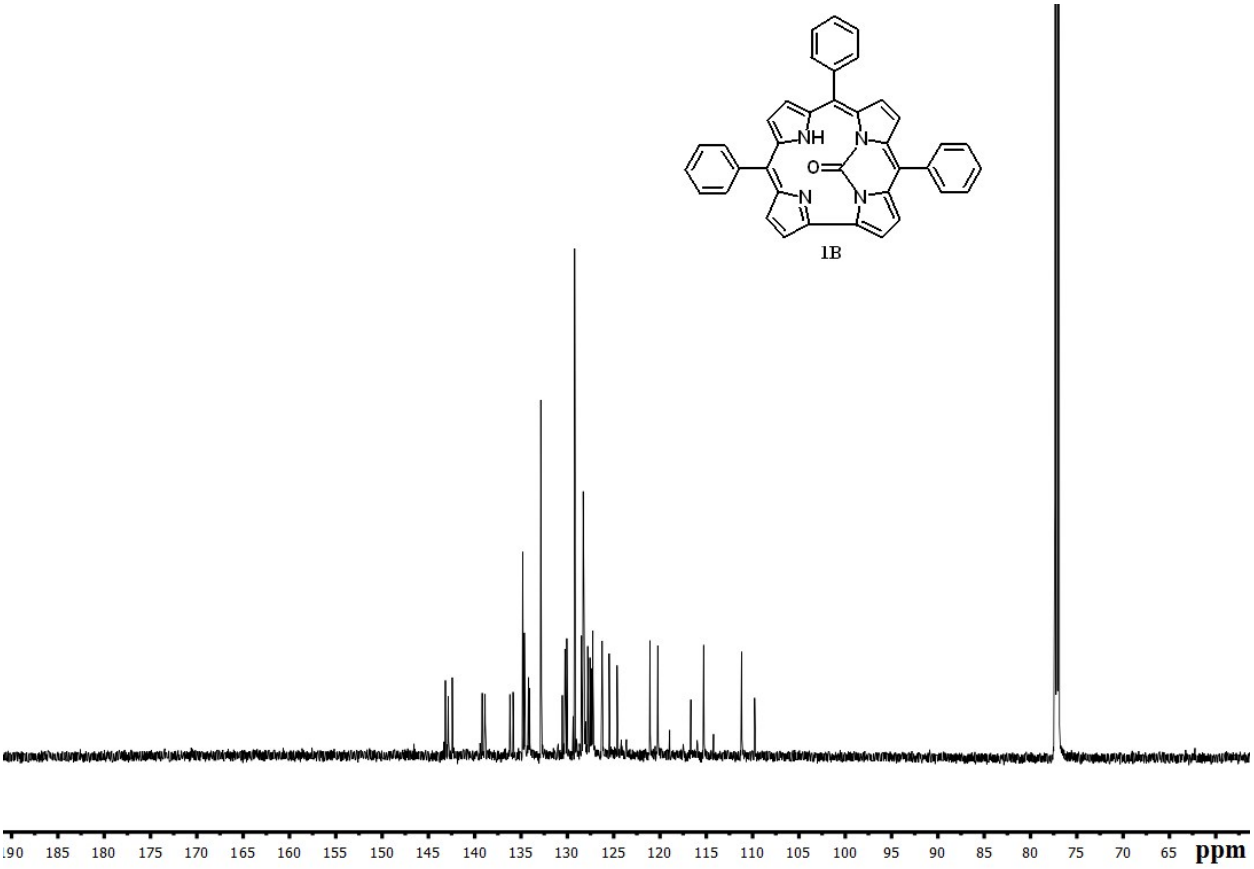

Fig. S2. ^{13}C NMR spectrum of **1B** in $CDCl_3$.

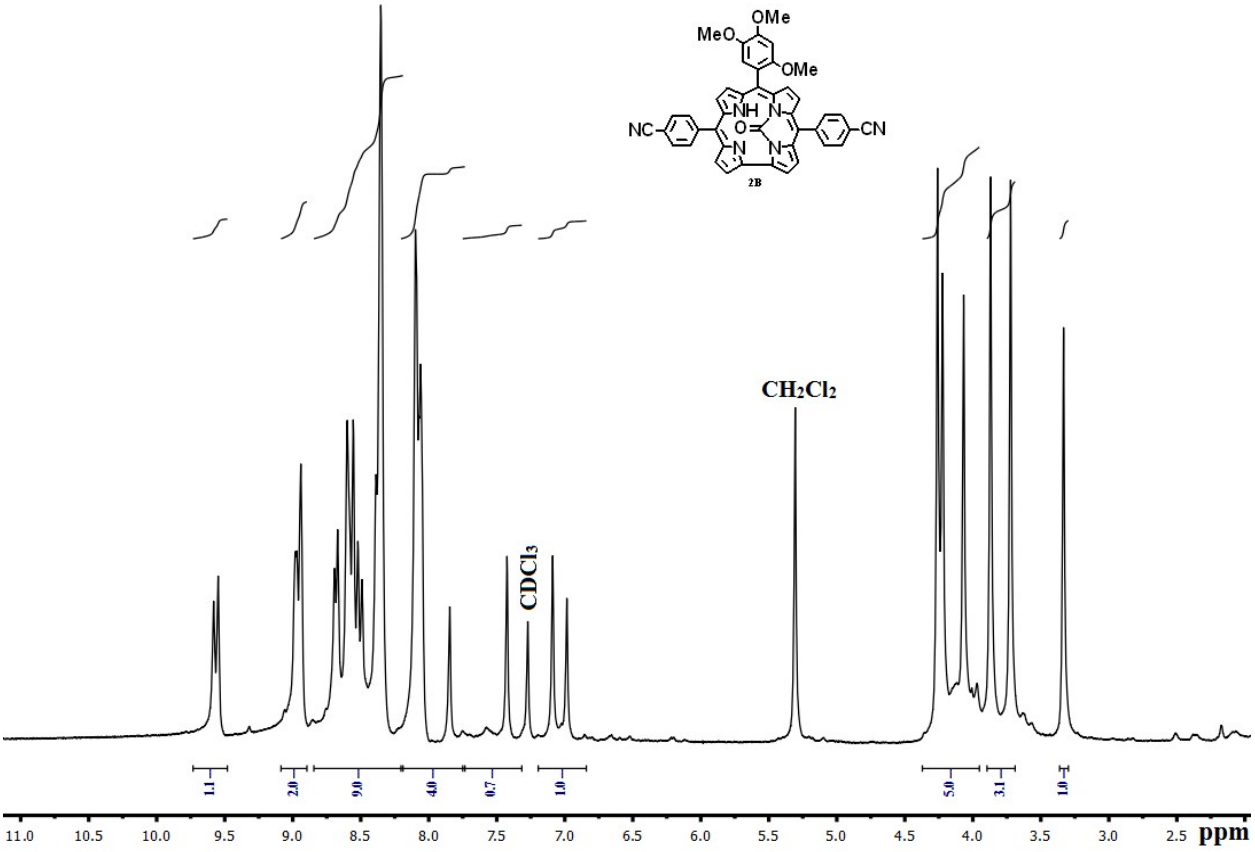

Fig. S3. ^{1}H NMR spectrum of **2B** in $CDCl_3$.

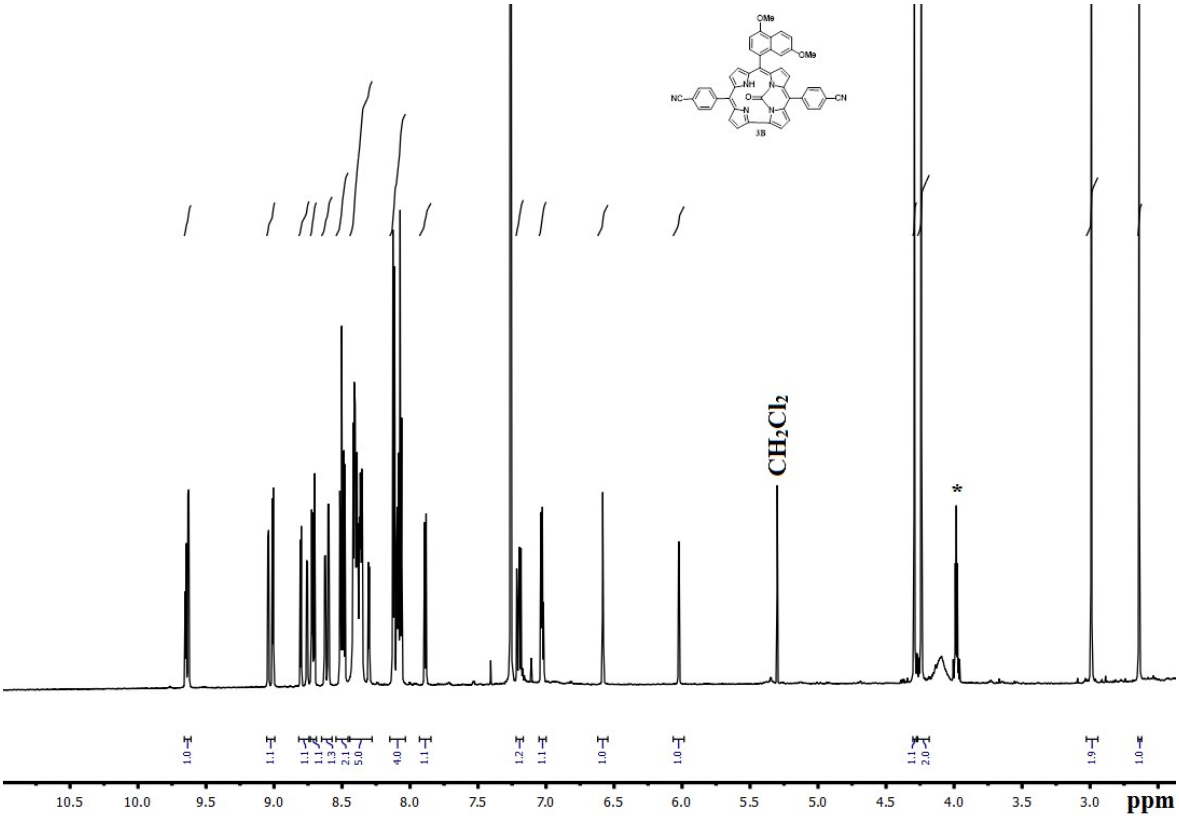

Fig. S4. ^{1}H NMR spectrum of **3B** in $CDCl_3$.

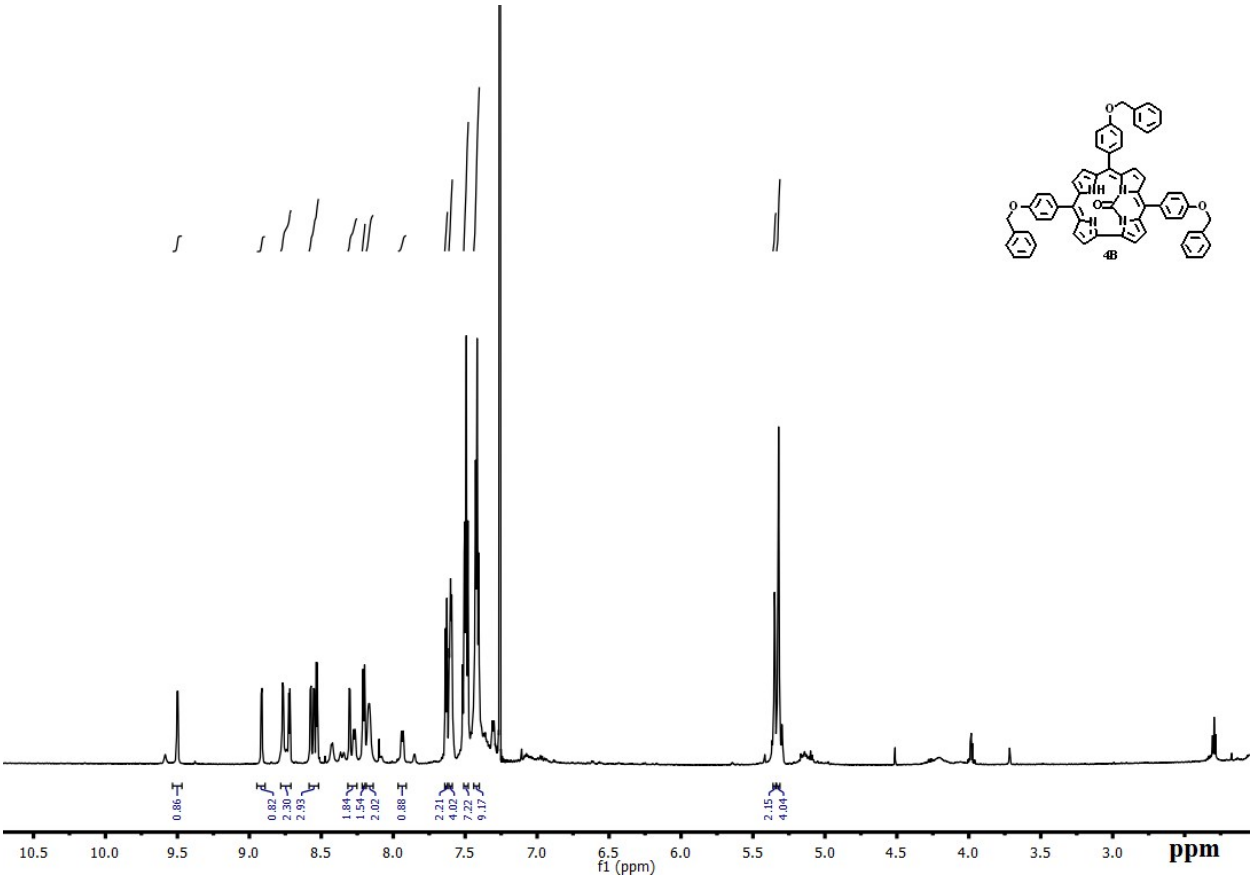

Fig. S5. ^{1}H NMR spectrum of **4B** in $CDCl_3$.

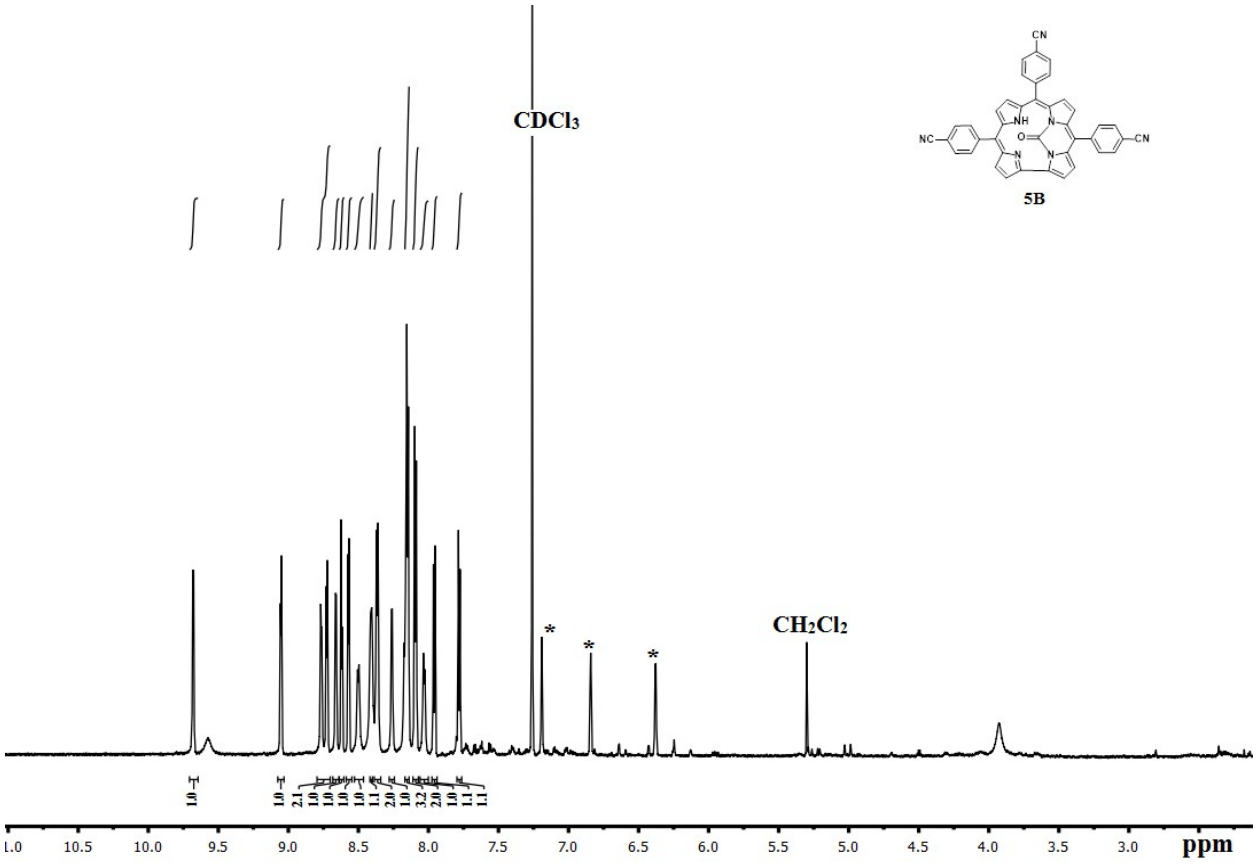

Fig. S6. ^{1}H NMR spectrum of **5B** in $CDCl_3$.

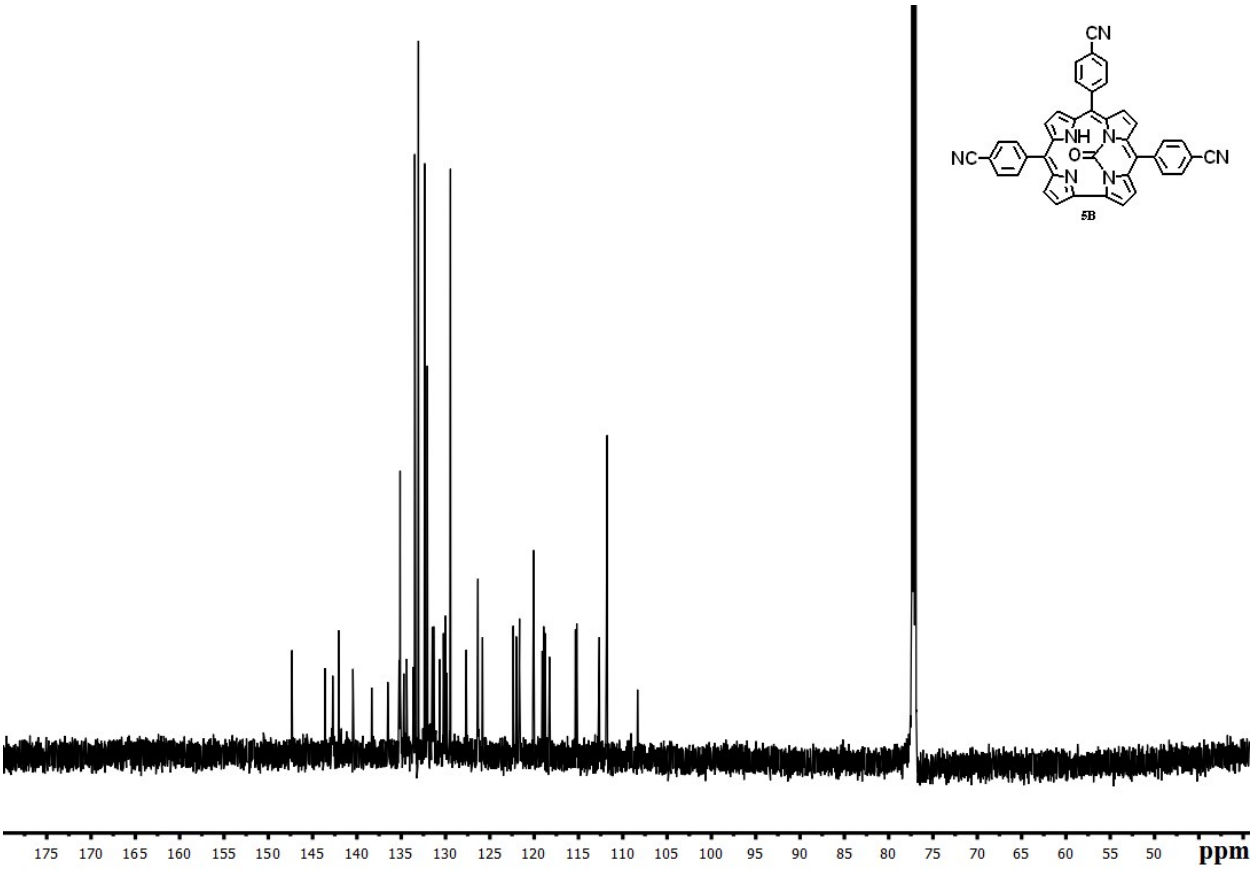

Fig. S7. ^{13}C NMR spectrum of **5B** in $CDCl_3$.

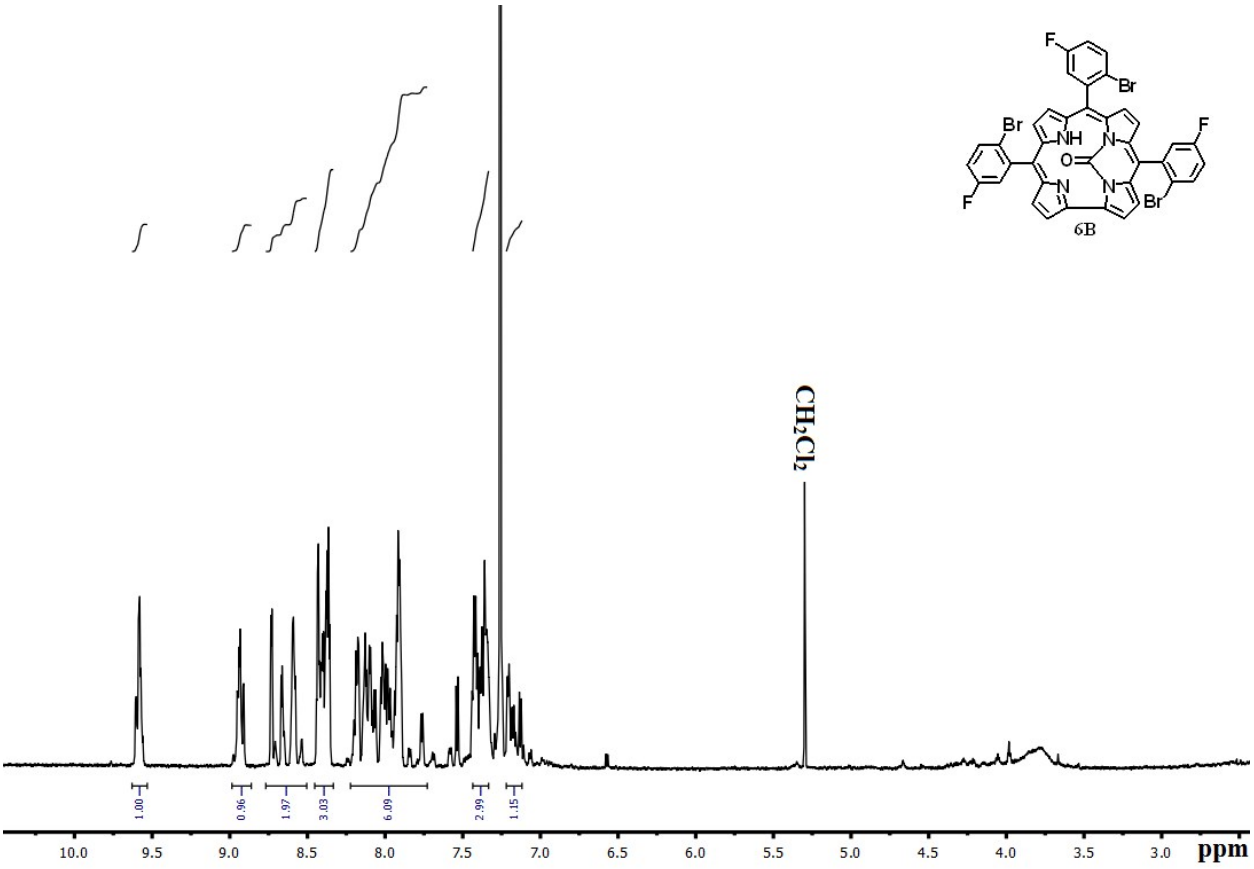

Fig. S8. ^{1}H NMR spectrum of **6B** in $CDCl_3$.

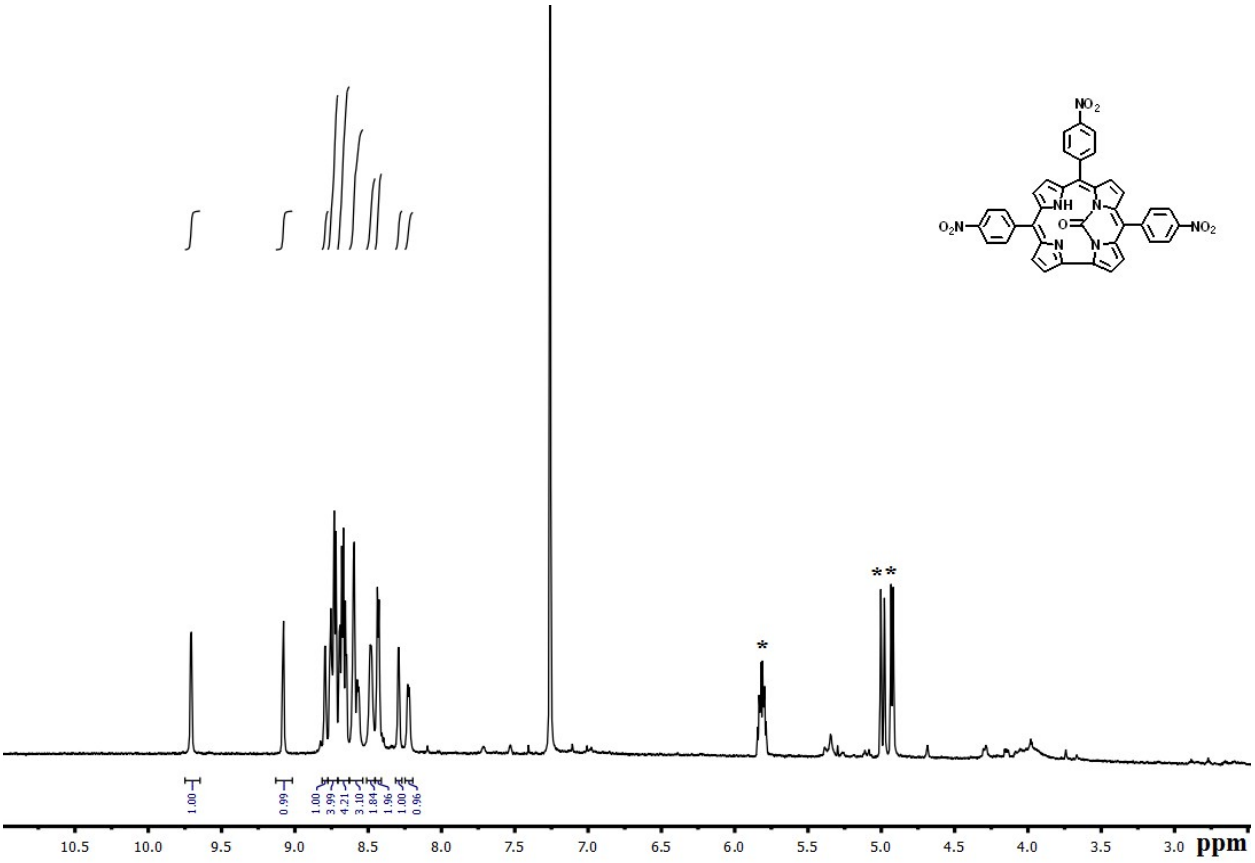

Fig. S9. ^{1}H NMR spectrum of **7B** in $CDCl_3$.

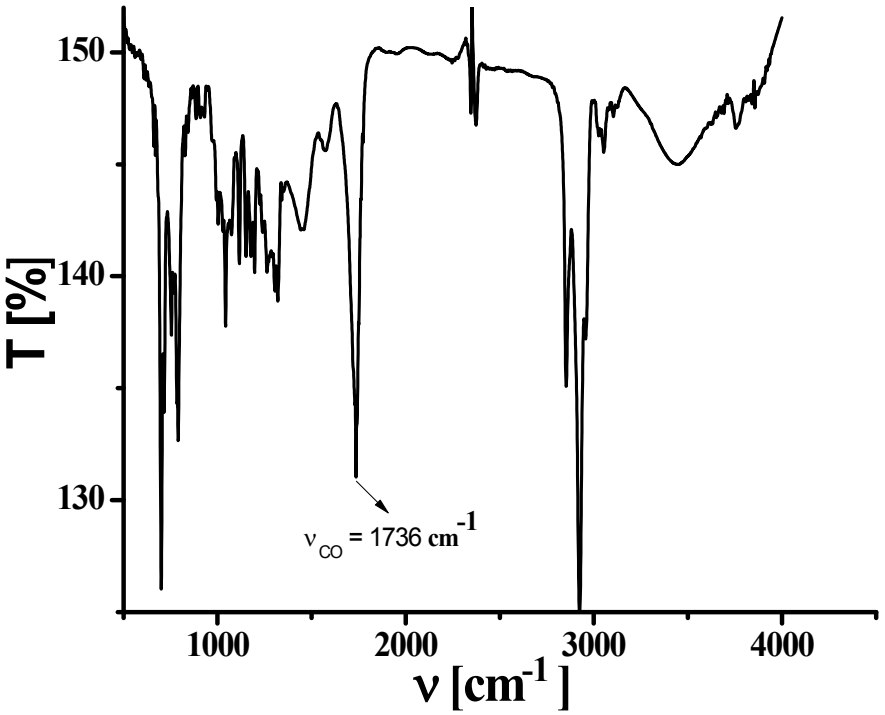

Fig. S10. FT-IR spectrum of **1B** as a KBr pellet.

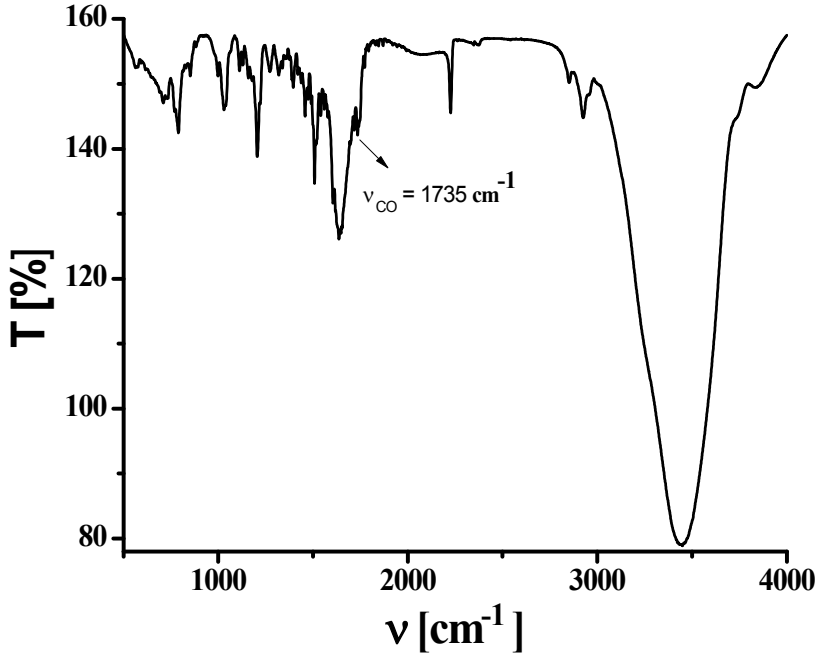

Fig. S11. FT-IR spectrum of **2B** as a KBr pellet.

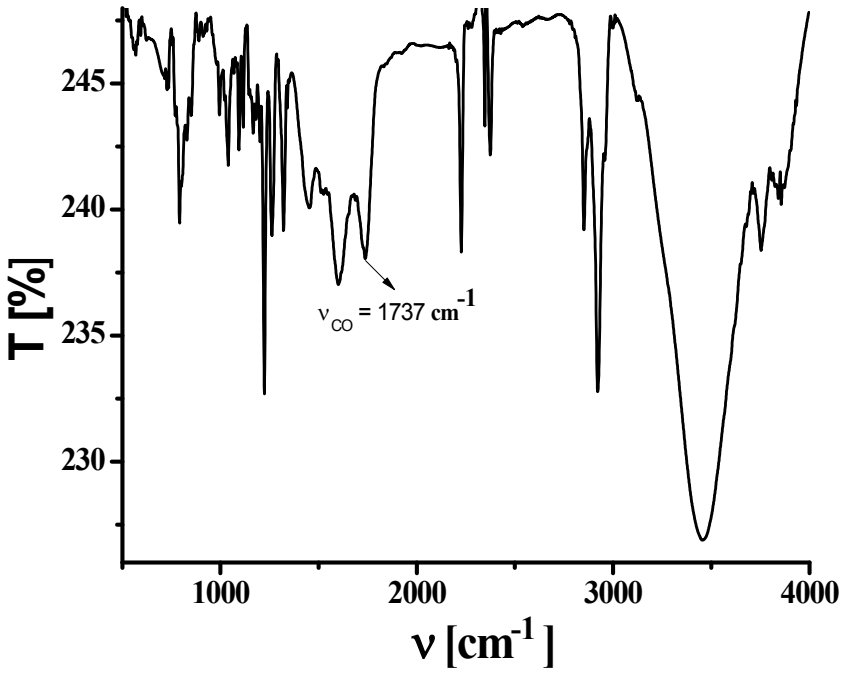

Fig. S12. FT-IR spectrum of **3B** as a KBr pellet.

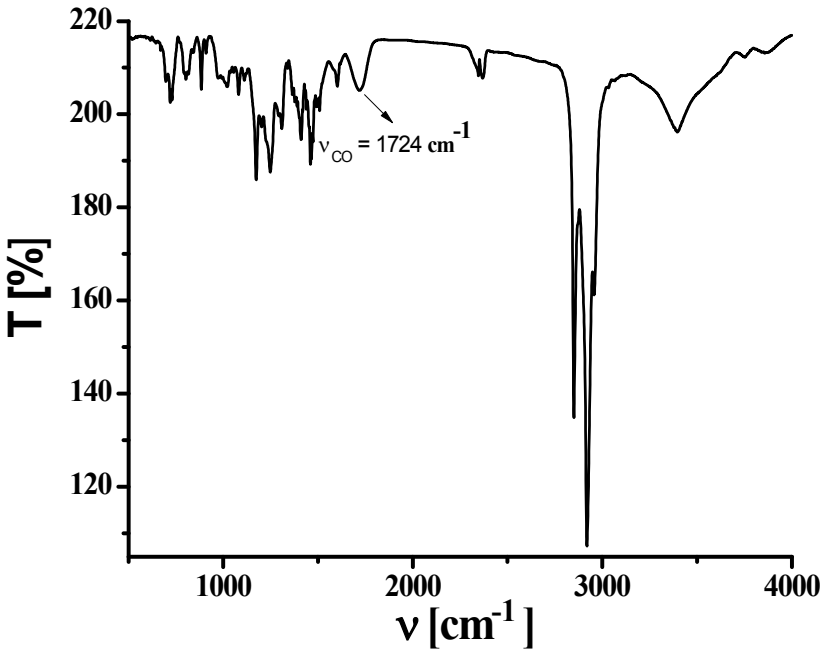

Fig. S13. FT-IR spectrum of **4B** as a KBr pellet.

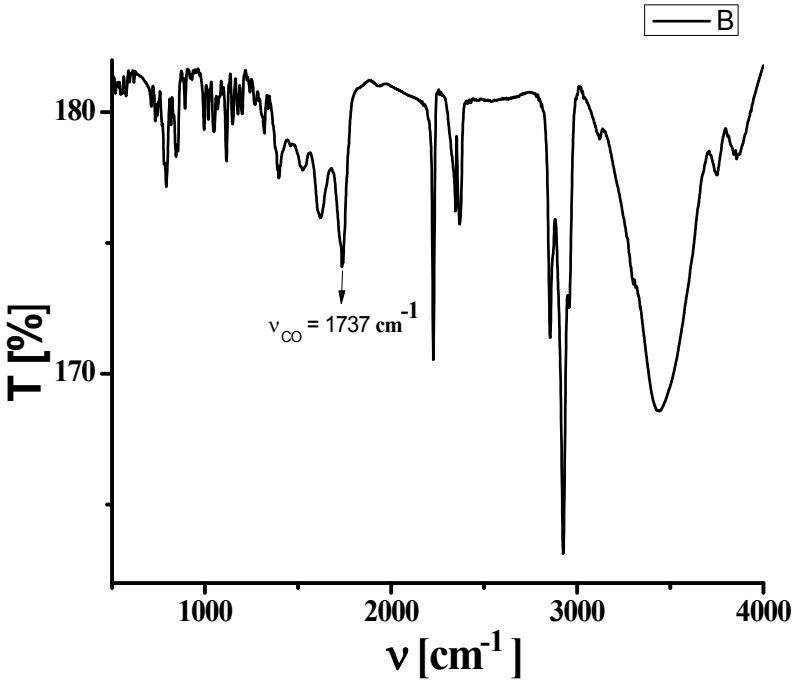

Fig. S14. FT-IR spectrum of **5B** as a KBr pellet.

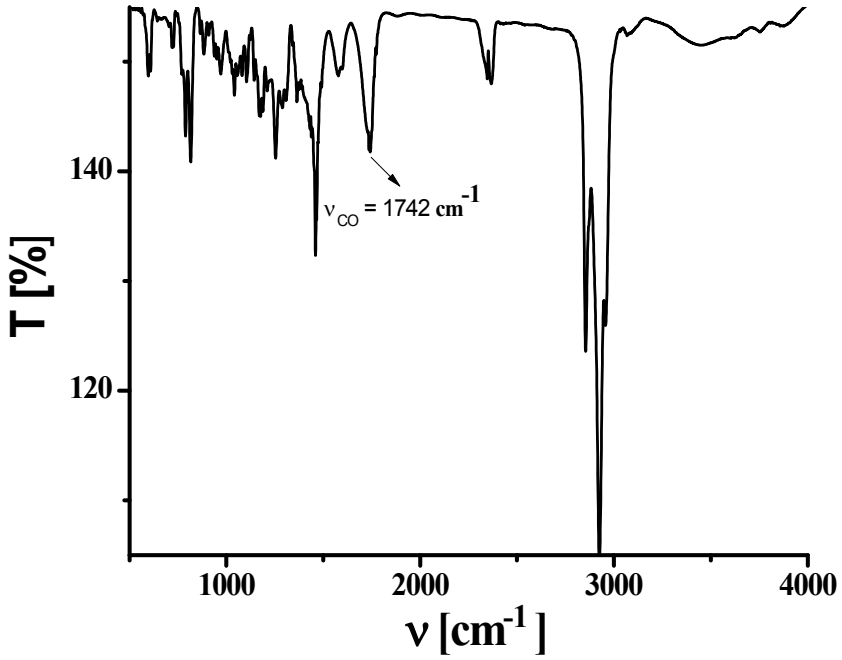

Fig. S15. FT-IR spectrum of **6B** as a KBr pellet.

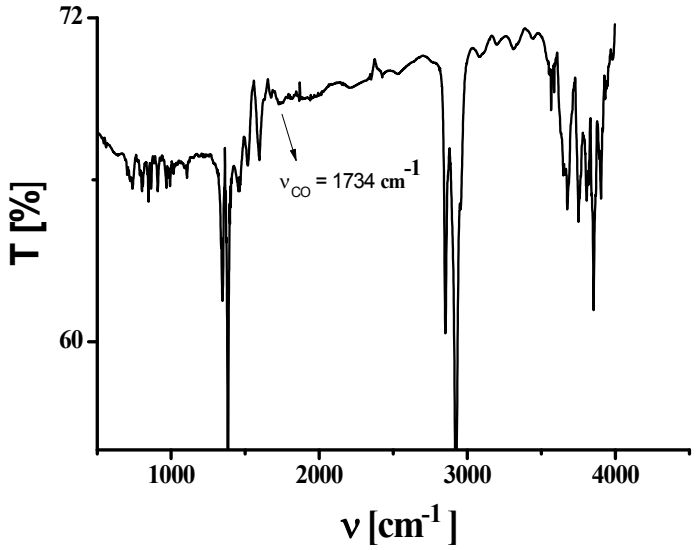

Fig. S16. FT-IR spectrum of **7B** as a KBr pellet.

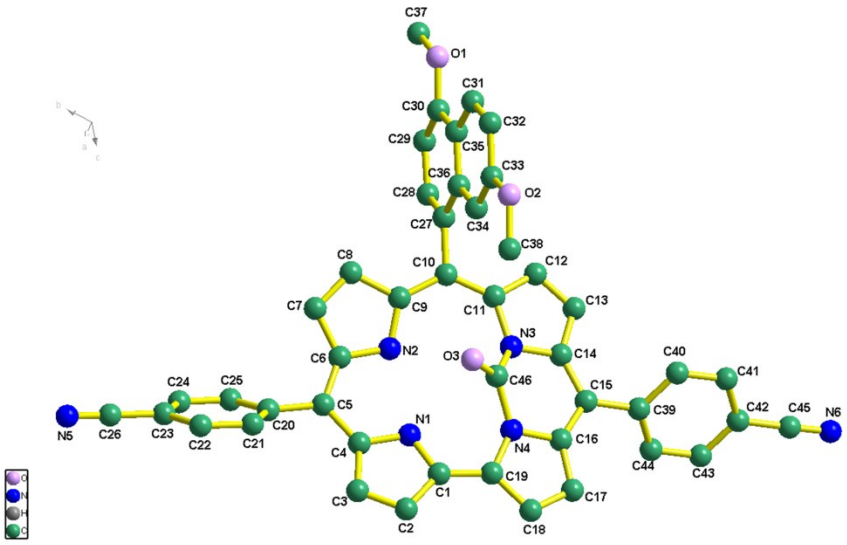

Fig. S17 Single-crystal X-ray structure of **3B.** Hydrogen atoms are omitted for clarity.

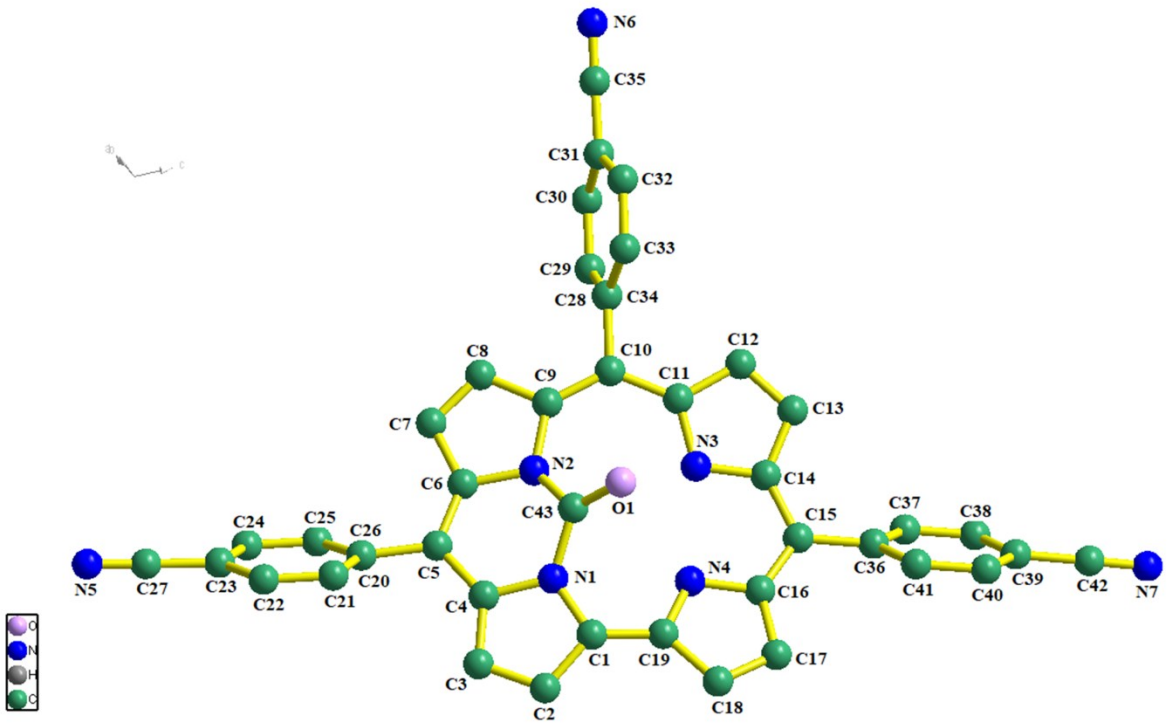

Fig. S18 Single-crystal X-ray structure of **5B.** Hydrogen atoms are omitted for clarity.

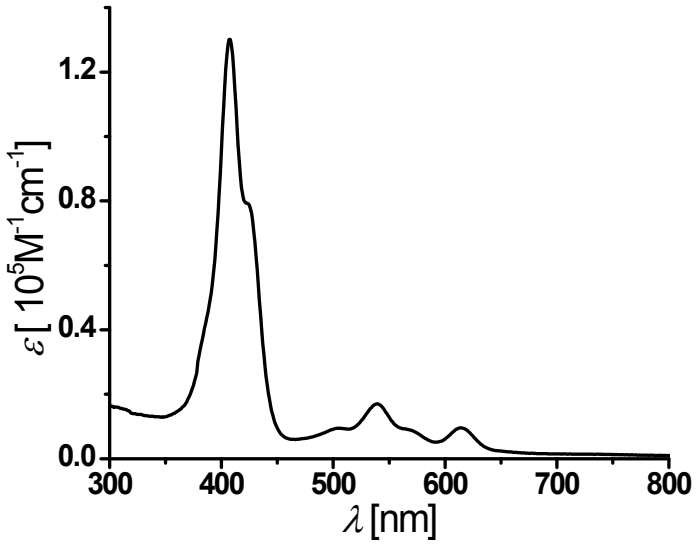

Fig. S19 Electronic absorption spectrum of **1B** in toluene.

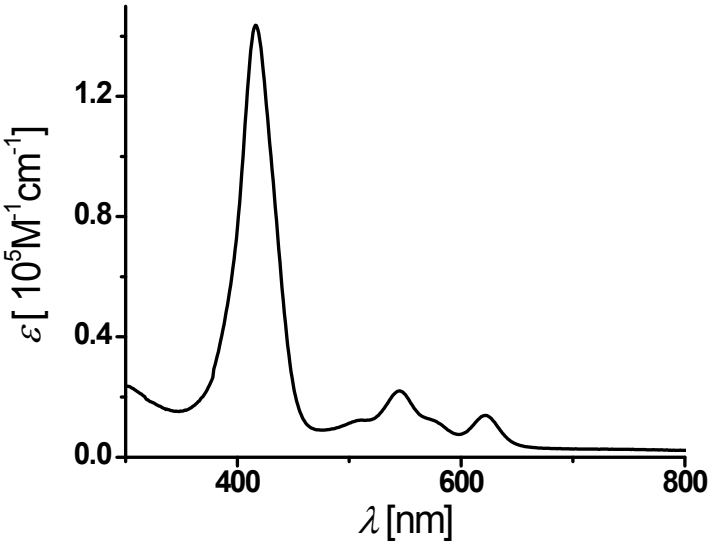

Fig. S20 Electronic absorption spectrum of **2B** in toluene.

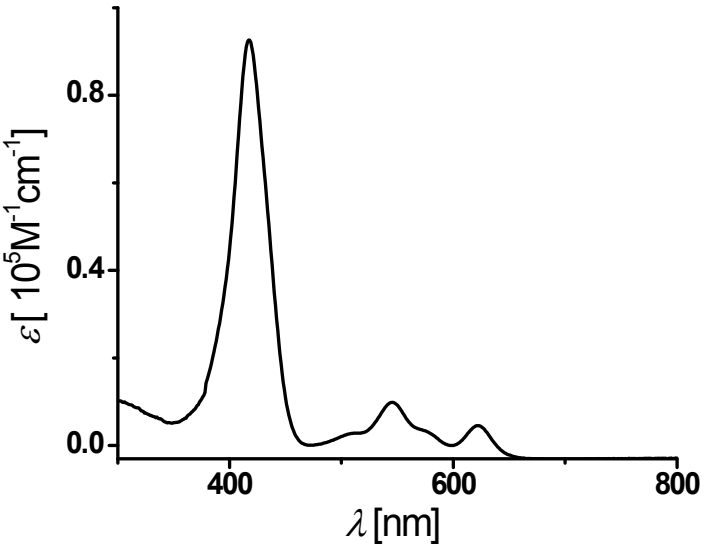

Fig. S21 Electronic absorption spectrum of **3B** in toluene.

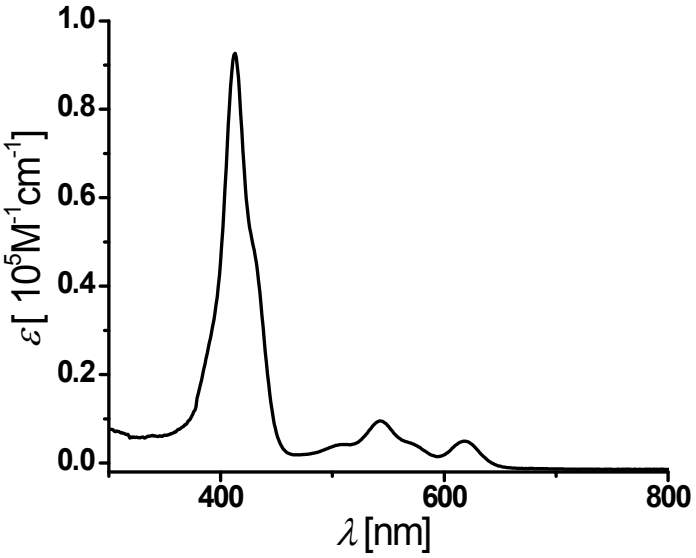

Fig. S22 Electronic absorption spectrum of **4B** in toluene.

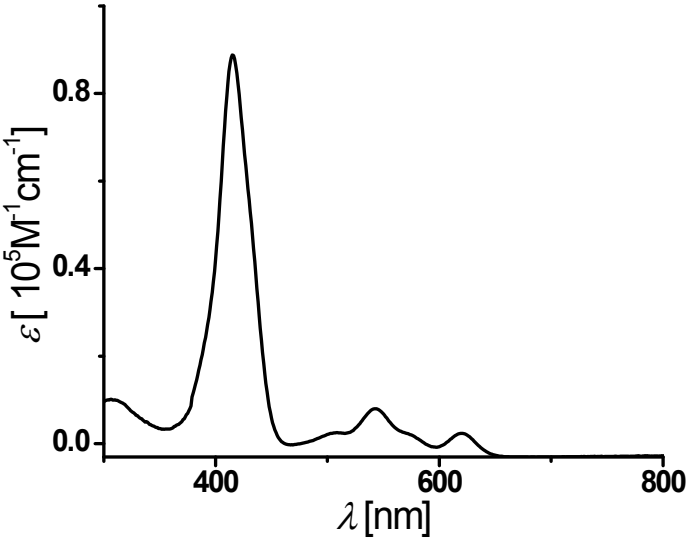

Fig. S23 Electronic absorption spectrum of **5B** in toluene.

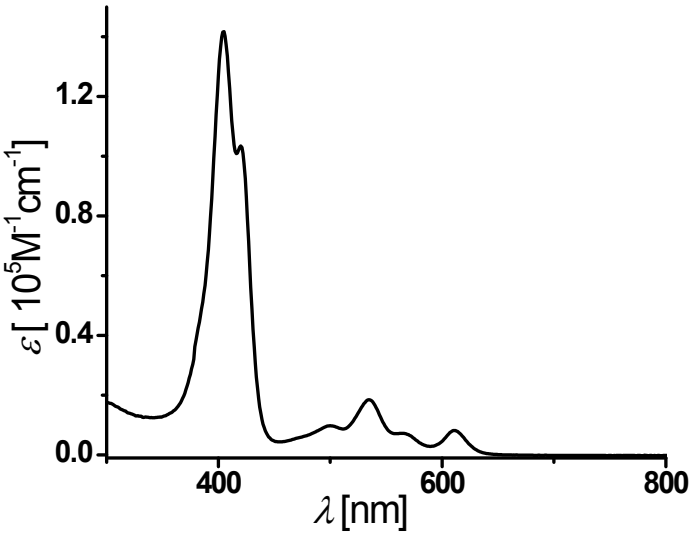

Fig. S24 Electronic absorption spectrum of **6B** in toluene.

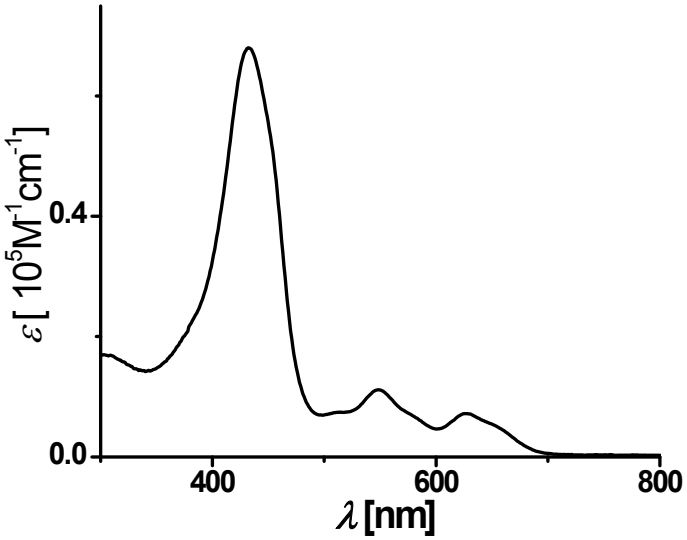

Fig. S25 Electronic absorption spectrum of **7B** in dichloromethane.

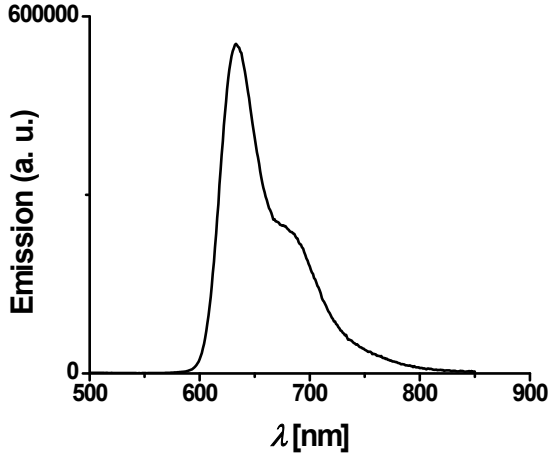

Fig. S26 Electronic emission spectrum (excited at the Soret band) of **1B** in toluene.

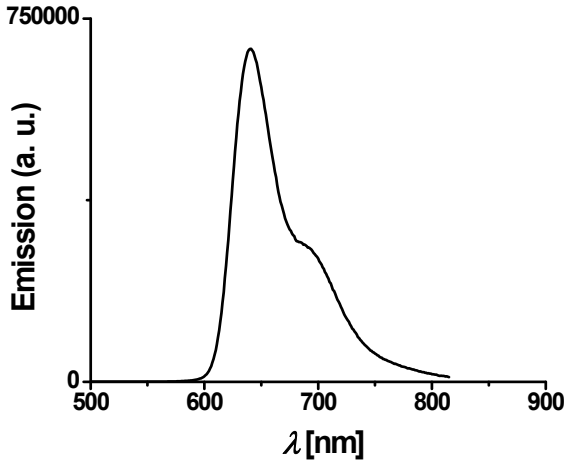

Fig. S27 Electronic emission spectrum (excited at the Soret band) of **2B** in toluene.

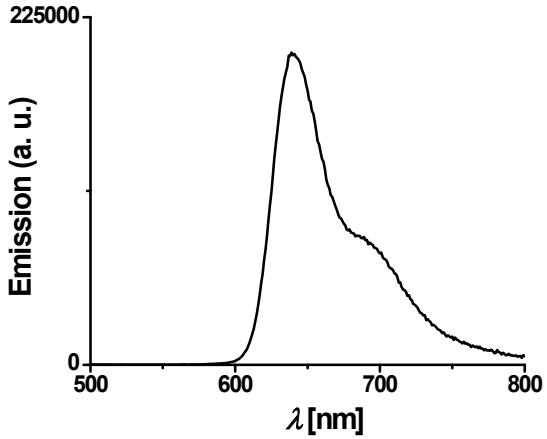

Fig. S28 Electronic emission spectrum (excited at the Soret band) of **3B** in toluene.

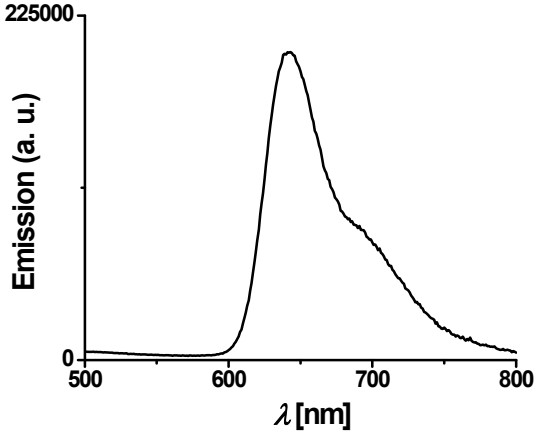

Fig. S29 Electronic emission spectrum (excited at the Soret band) of **4B** in toluene.

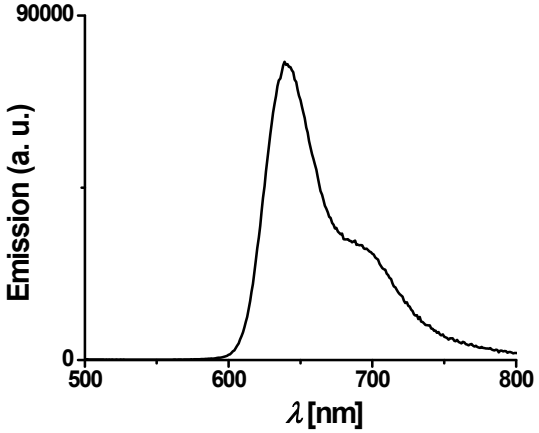

Fig. S30 Electronic emission spectrum (excited at the Soret band) of **5B** in toluene.

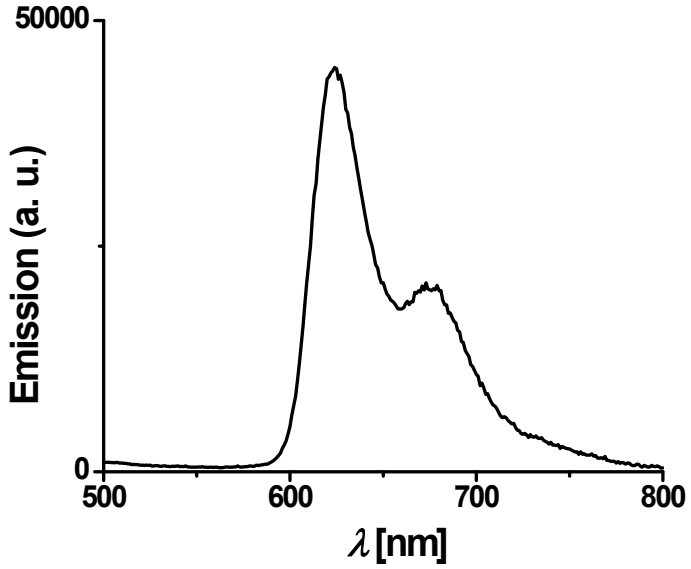

Fig. S31 Electronic emission spectrum (excited at the Soret band) of **6B** in toluene.

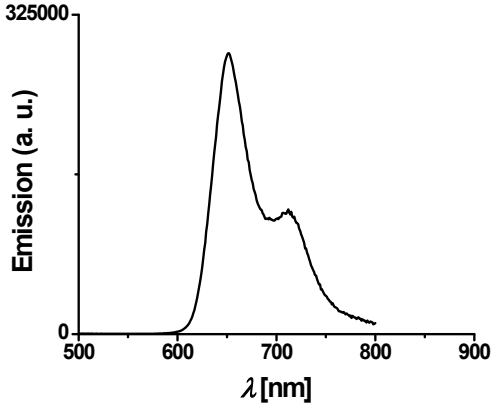

Fig. S32 Electronic emission spectrum (excited at the Soret band) of **7B** in toluene.

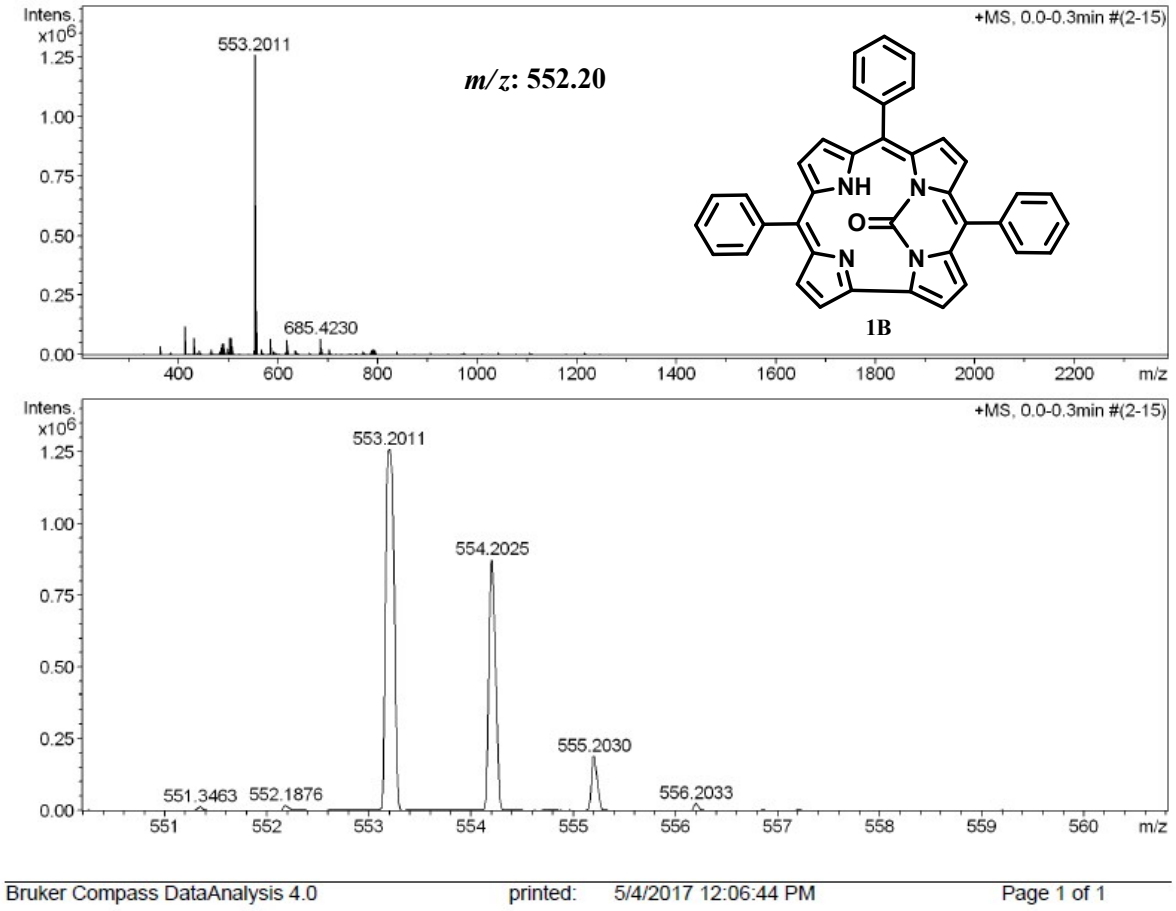

Fig. S33. ESI- MS spectrum of **1B** in CH_3CN shows the measured spectrum with isotopic distribution pattern.

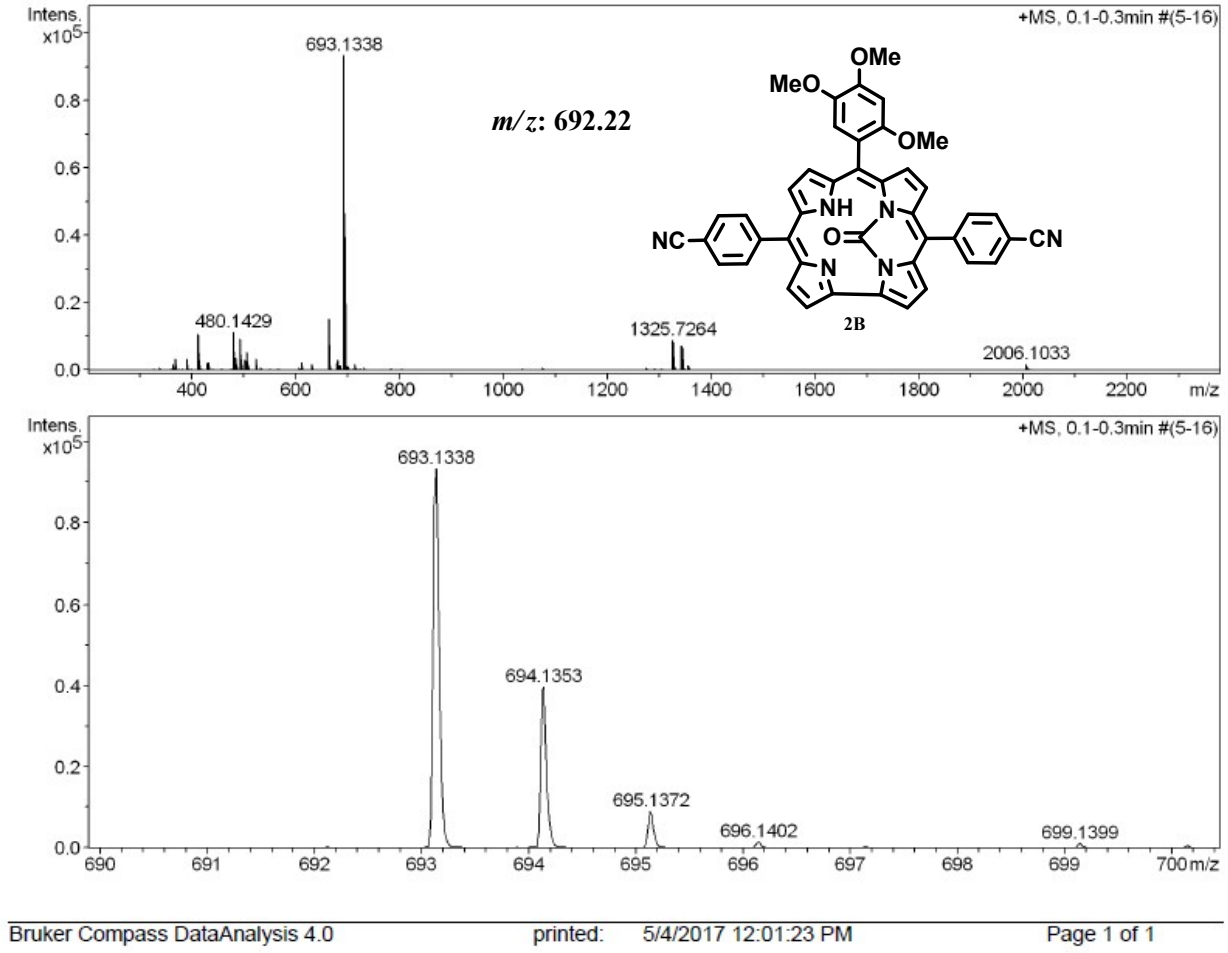

Fig. S34. ESI- MS spectrum of **2B** in CH_3CN shows the measured spectrum with isotopic distribution pattern.

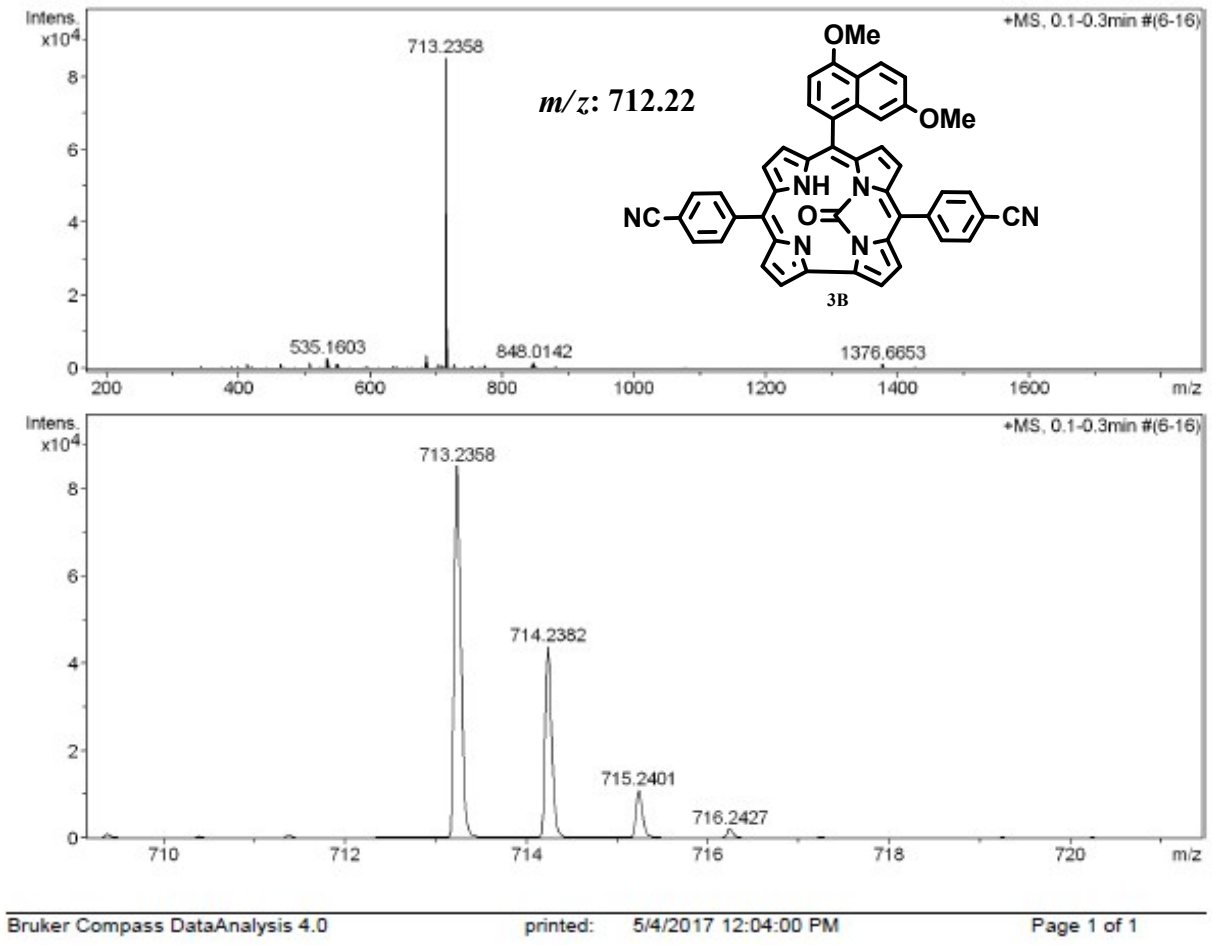

Fig. S35. ESI- MS spectrum of **3B** in CH_3CN shows the measured spectrum with isotopic distribution pattern.

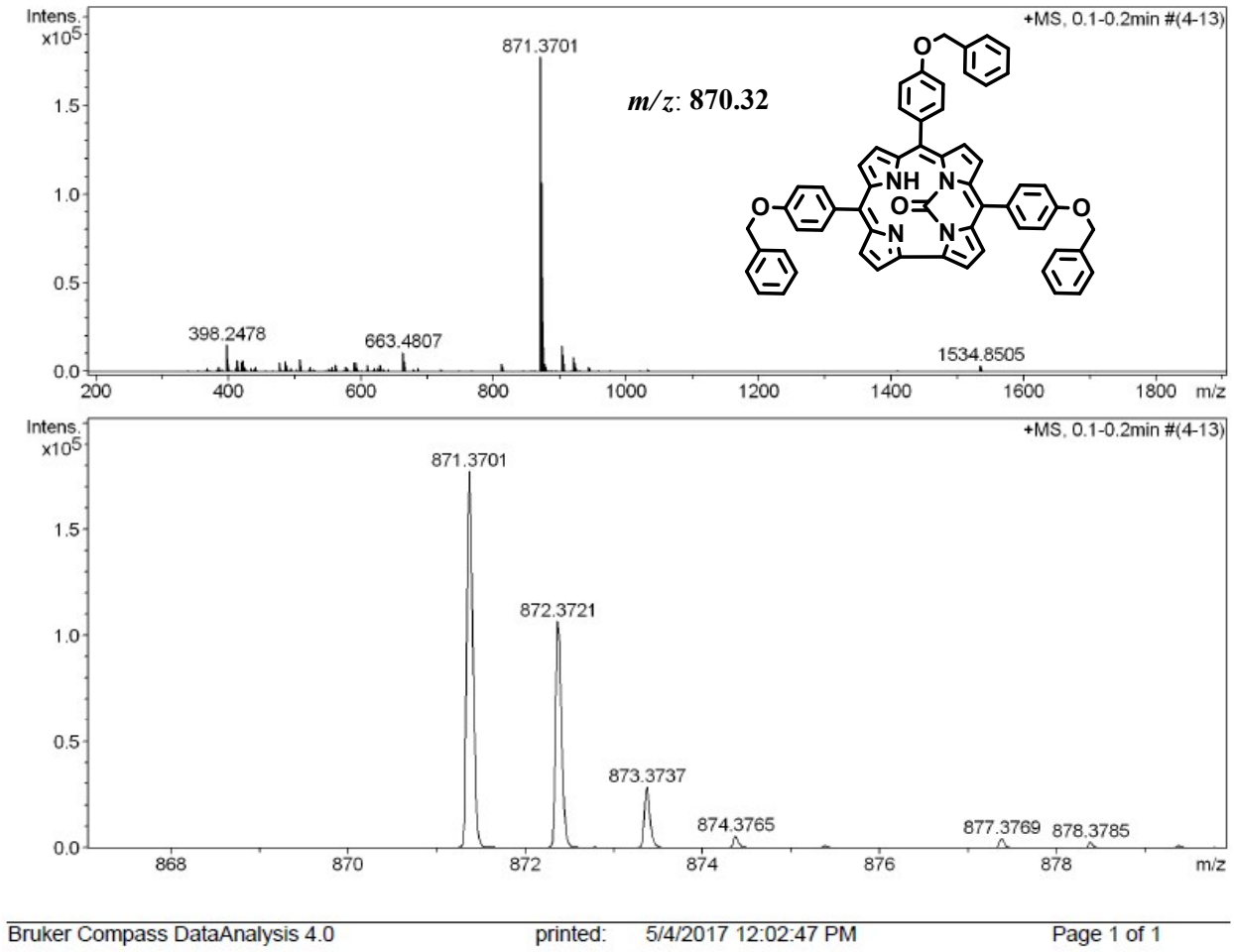

Fig. S36. ESI- MS spectrum of **4B** in CH_3CN shows the measured spectrum with isotopic distribution pattern.

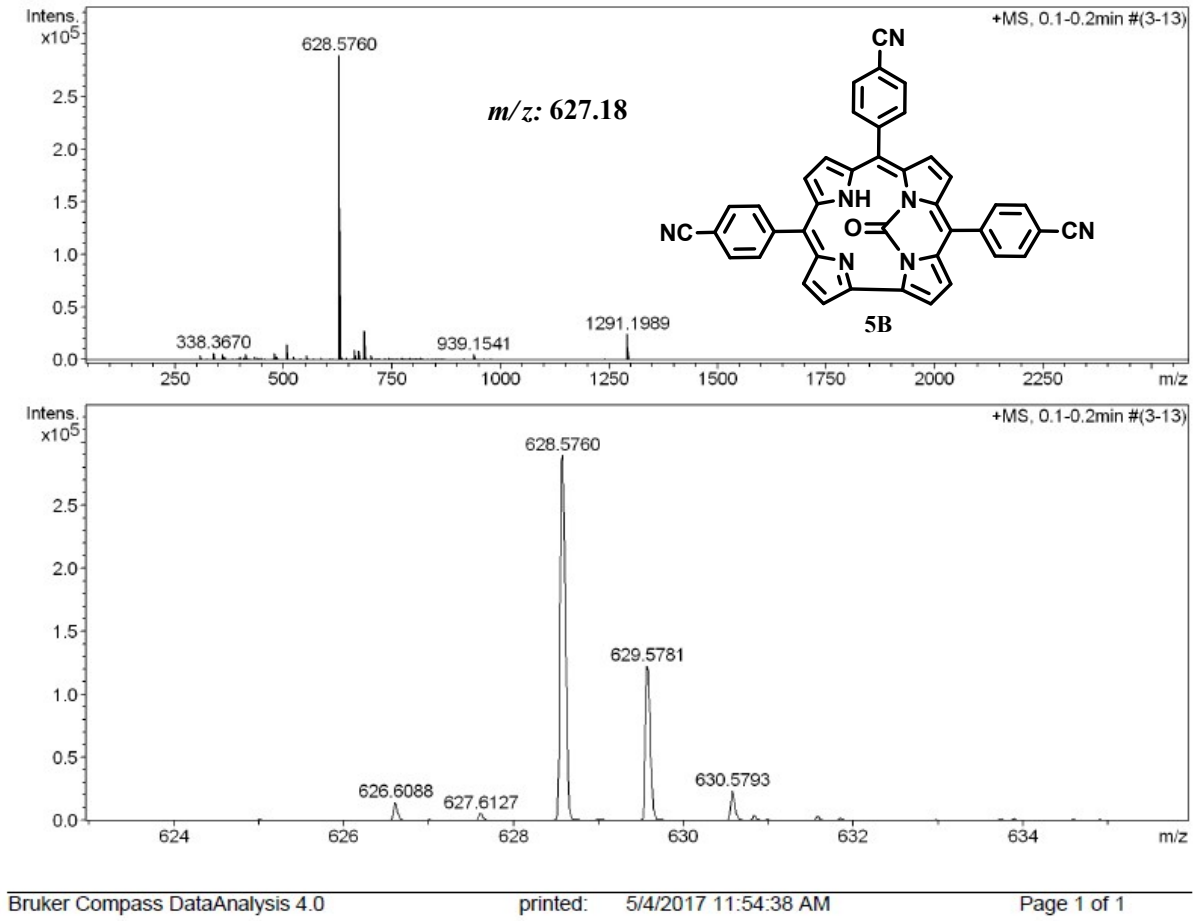

Fig. S37. ESI- MS spectrum of **5B** in CH_3CN shows the measured spectrum with isotopic distribution pattern.

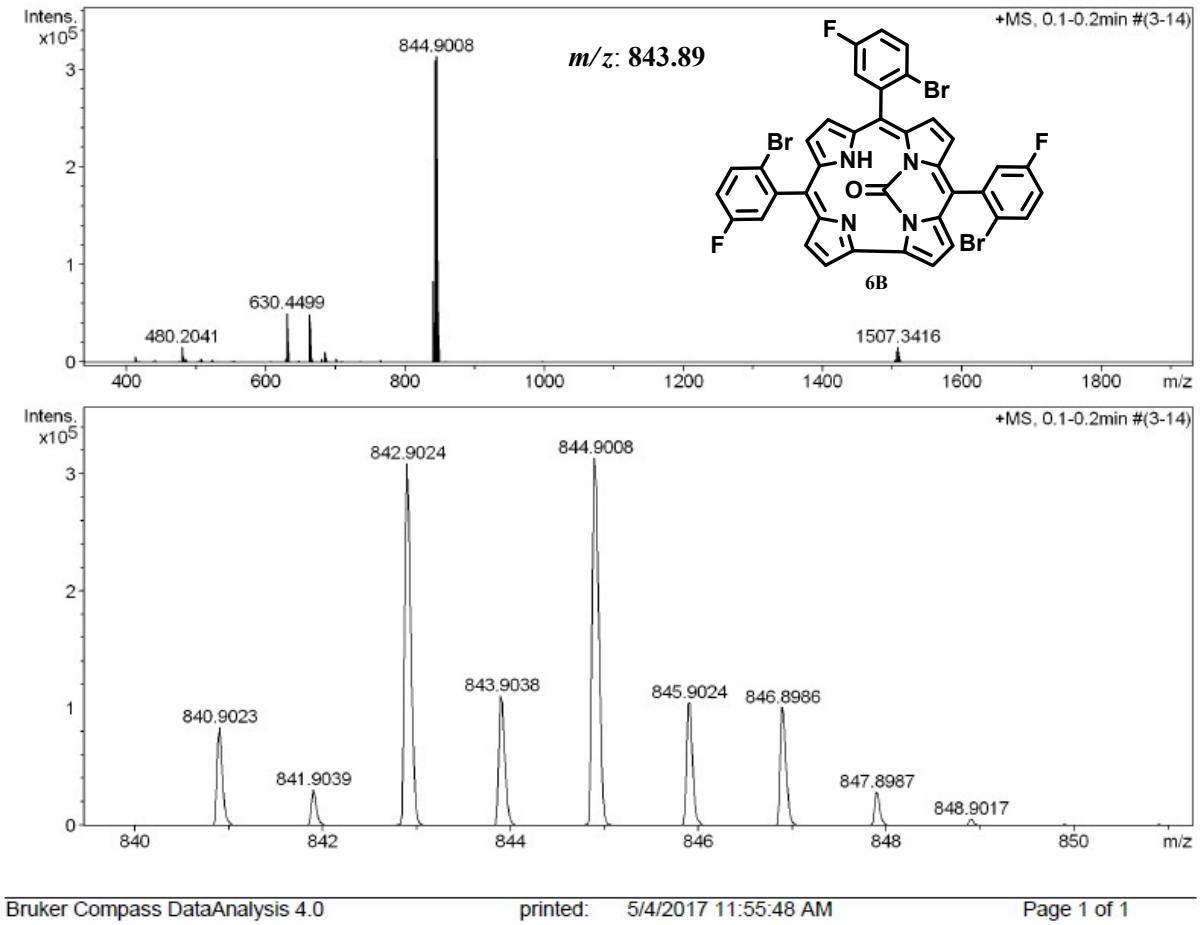

6B

Fig. S38. ESI- MS spectrum of **6B** in CH_3CN shows the measured spectrum with isotopic distribution pattern.

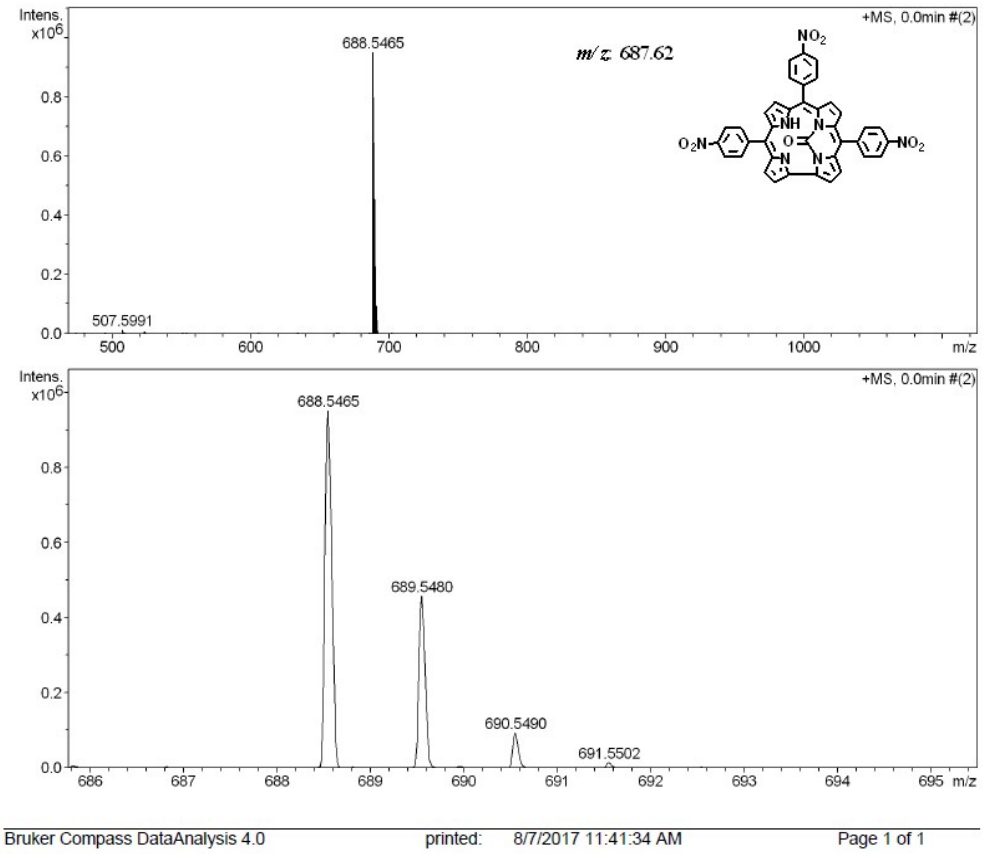

Fig. S39. ESI- MS spectrum of **7B** in CH_3CN shows the measured spectrum with isotopic distribution pattern.

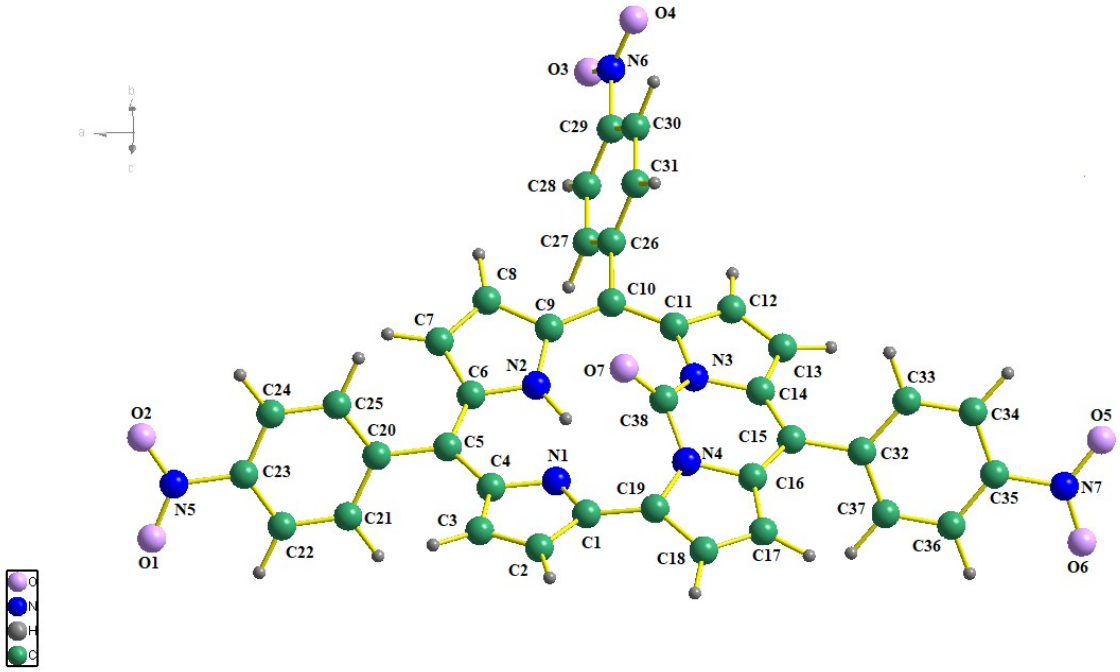

Figure S40. DFT optimized (B97-D/6-31G*) structures of **7B**.